

Arbeitsbericht

NAB 21-20

TBO Marthalen-1-1:
Data Report
Dossier X
Petrophysical Log Analysis

September 2021

S. Marnat & J.K. Becker

National Cooperative
for the Disposal of
Radioactive Waste

Hardstrasse 73
P.O. Box 280
5430 Wettingen
Switzerland
Tel. +41 56 437 11 11

www.nagra.ch

Arbeitsbericht

NAB 21-20

TBO Marthalen-1-1:
Data Report

Dossier X
Petrophysical Log Analysis

September 2021

S. Marnat¹ & J.K. Becker²

¹ GPCI

² Nagra

Keywords:

MAR1-1, Zürich Nordost, TBO, deep drilling campaign,
stochastic log interpretation, MultiMin analyses,
petrophysical logs, lab data, Multi-Sensor Core Logger,
MSCL, mineralogy, clay content, clay typing, porosity

**National Cooperative
for the Disposal of
Radioactive Waste**

Hardstrasse 73
P.O. Box 280
5430 Wettingen
Switzerland
Tel. +41 56 437 11 11

www.nagra.ch

Nagra Arbeitsberichte ("Working Reports") present the results of work in progress that have not necessarily been subject to a comprehensive review. They are intended to provide rapid dissemination of current information.

This NAB aims at reporting drilling results at an early stage. Additional borehole-specific data will be published elsewhere.

In the event of inconsistencies between dossiers of this NAB, the dossier addressing the specific topic takes priority. In the event of discrepancies between Nagra reports, the chronologically later report is generally considered to be correct. Data sets and interpretations laid out in this NAB may be revised in subsequent reports. The reasoning leading to these revisions will be detailed there.

This Dossier was prepared by a project team consisting of:

S. Marnat (data analyses, interpretation and writing)

J.K. Becker (project administration and writing)

Editorial work: P. Blaser and M. Unger

The Dossier has greatly benefitted from technical discussions with, and reviews by, internal experts. Their input and work are very much appreciated.

"Copyright © 2021 by Nagra, Wettingen (Switzerland) / All rights reserved.

All parts of this work are protected by copyright. Any utilisation outwith the remit of the copyright law is unlawful and liable to prosecution. This applies in particular to translations, storage and processing in electronic systems and programs, microfilms, reproductions, etc."

Table of Contents

Table of Contents	I
List of Tables.....	II
List of Figures	II
List of Appendices	III
List of Plates.....	III
Abbreviations	IV
1 Introduction	1
1.1 Context.....	1
1.2 Location and specifications of the borehole	2
1.3 Documentation structure for the MAR1-1 borehole.....	6
1.4 Scope and objectives of this dossier	7
2 Data preparation.....	9
2.1 Used log data	9
2.2 Used core data	12
2.3 Multi-sensor Core Logger (MSCL) data	12
2.4 MultiMin input dataset preparation	15
2.5 Preliminary calculations (Precalc).....	15
3 Petrophysical log interpretation	17
3.1 MultiMin interpretation	17
3.2 Bad-hole treatment and quality of results.....	19
3.2.1 Indicator for input data quality (LQC_INDEX)	19
3.2.2 Indicator for the mathematical model (CONDNUM and NFUN).....	20
3.2.3 Indicator for the MultiMin interpretation results (MULT_QC and QUALITY)	20
4 Results of the calibrated stochastic log interpretation	23
4.1 Comparison of interpretation results with core data.....	23
4.2 Main results of the core-calibrated log analysis in borehole MAR1-1	31
4.3 Main results of the core-calibrated log analysis in the Opalinus Clay (590.4 – 705.5 m).....	36
5 Summary	45
6 References.....	47

List of Tables

Tab. 1-1:	General information about the MAR1-1 borehole.....	2
Tab. 1-2:	Core and log depth for the main lithostratigraphic boundaries in the MAR1-1 borehole	5
Tab. 1-3:	List of dossiers included in NAB 21-20	6
Tab. 3-1:	List of MultiMin models used in MAR1-1.....	18

List of Figures

Fig. 1-1:	Tectonic overview map with the three siting regions under investigation	1
Fig. 1-2:	Overview map of the investigation area in the Zürich Nordost siting region with the location of the MAR1-1 borehole in relation to the boreholes Benken, Schlattingen-1 and TRU1-1	3
Fig. 1-3:	Lithostratigraphic profile and casing scheme for the MAR1-1 borehole	4
Fig. 2-1:	Petrophysical log availability and gaps in the borehole MAR1-1	11
Fig. 2-2:	XRF (black dots) and ECS WALK2 (red curves) elements comparison.....	13
Fig. 2-3:	Core (black dots: Spectral Gamma Ray, blue dots: XRF thorium) and wireline HNGS (red curves) Spectral Gamma Ray elements comparison	14
Fig. 4-1:	Weight % of dry clay (y-axis) compared to core XRD data (x-axis), Villigen to Weitenau Formations.....	24
Fig. 4-2:	Weight % of not potassic dry clay (y-axis) compared to core XRD data (x-axis), XRD data in the Variansmergel to the Kaiseraugst Formations	25
Fig. 4-3:	Weight of illite (x axis) compared to core XRD data (y axis), XRD data in the Variansmergel to the Kaiseraugst Formations	26
Fig. 4-4:	Weight % of QF-silicates (x axis) compared to core XRD data (y axis), Villigen to Weitenau Formations.....	27
Fig. 4-5:	Weight % of carbonates (x axis) compared to core XRD data (y axis), Villigen to Weitenau Formations.....	28
Fig. 4-6:	Weight % of dolomite (x axis) compared to core XRD data (y axis), Villigen to Weitenau Formations.....	29
Fig. 4-7:	Total porosity (v/v, y axis) compared to core data (x axis), Villigen to Weitenau Formations.....	30
Fig. 4-8:	Bulk density computed from core grain density and water loss porosity versus RHOZ in the «Brauner Dogger»	33
Fig. 4-9:	Dry clay weight percentage frequency histogram in the Opalinus Clay.....	37
Fig. 4-10:	Dry clay weight percentage frequency histogram in the upper section of the Opalinus Clay (above 659 m)	38

Fig. 4-11:	Dry clay weight percentage frequency histogram in the lower section of the Opalinus Clay (below 659 m).....	39
Fig. 4-12:	Calcite weight percentage frequency histogram in the Opalinus Clay	40
Fig. 4-13:	Siderite weight percentage frequency histogram in the Opalinus Clay	41
Fig. 4-14:	QF-silicates (quartz and feldspars) weight percentage frequency histogram in the Opalinus Clay	42
Fig. 4-15:	Total porosity frequency histogram in the Opalinus Clay	43
Fig. 4-16:	Main log and core results in the Opalinus Clay.....	44

List of Appendices

- App. A: Precalc parameters table
- App. B: List of MultiMin models
- App. C: Parameters used in the different MultiMin models

List of Plates

- Plate 1: Comparison of calculated log curves and measured petrophysical log curves
- Plate 2: Results of the core-calibrated petrophysical log interpretation

Note: In the digital version of this report the appendices and plates can be found under the paper clip symbol.

Abbreviations

ANHYDR	Anhydrite weight percentage from MultiMin
APLC	Corrected neutron hydrogen index from APS (limestone matrix)
APLC_PRED	APLC prediction by MultiMin
APS	Accelerator Porosity Sonde
B/E	Barns/Electron
BS	Drilling / Coring Bit Size
CALCITE	Calcite weight percentage from MultiMin
CALI	Caliper
CARBONATES	Carbonates weight percentage from MultiMin
CHLORITE	Chlorite weight percentage from MultiMin
COAL	Coal weight percentage from MultiMin
COMPOSITE	Composite log, validated logs dataset
CONDNUM	MultiMin model condition number
CT	Conductivity in the formation
CT_PRED	CT prediction by MultiMin
CU	Capture Unit, unit for sigma
CXO	Conductivity in the invaded zone
CXO_PRED	CXO prediction by MultiMin
DENS	Bulk density
DOLOMITE	Dolomite weight percentage from MultiMin
DRHO	Bulk density correction
DRY_CLAY	Dry clay weight percentage from MultiMin
dRRC	Rush raw corrected data
DWAL_WALK2	Dry weight fraction aluminium, ECS WALK2 closure model
DWCA_WALK2	Dry weight fraction calcium, ECS WALK2 closure model
DWFE_WALK2	Dry weight fraction iron, ECS WALK2 closure model
DWFE_CORR	Dry weight fraction iron, calibrated to XRF iron content
DWSI_WALK2	Dry weight fraction silicon, ECS WALK2 closure model
DWSU_WALK2	Dry weight fraction sulphur, ECS WALK2 closure model
DWTI_WALK2	Dry weight fraction titanium from ECS, ECS WALK2 closure model

DWAL_MGWALK	Dry weight fraction aluminium, ECS MGWALK closure model
DWCA_MGWALK	Dry weight fraction calcium, ECS MGWALK closure model
DWFE_MGWALK	Dry weight fraction iron, ECS MGWALK closure model
DWSI_MGWALK	Dry weight fraction silicon, ECS MGWALK closure model
DWSU_MGWALK	Dry weight fraction sulphur, ECS MGWALK closure model
DWTI_MGWALK	Dry weight fraction titanium, ECS MGWALK closure model
DWMG_MGWALK	Dry weight fraction magnesium, ECS MGWALK closure model
DTCO	Compressional wave slowness from far monopole mid frequency source compressional wave slowness
DTCO_PRED	DTCO prediction by MultiMin
DTSM	Shear wave slowness from inline X-Dipole (90°) source
DTSM_PRED	DTSM prediction by MultiMin
ECS	Elemental Capture Spectroscopy
ECS WT.-%	Weight percent
EDTC	Enhanced Digital Telemetry Cartridge
EMS	Environment Measurement Sonde
FE_MIN	Iron-rich minerals (siderite, pyrite, iron oxides)
FLAG_BADHOLE_DN	Badhole flag from the Density-Neutron crossplot
FLAG_BADHOLE_OVERGAUGE	Badhole flag from the Caliper
FLAG_BADHOLE_RUGO	Badhole flag from the Density correction
FLAG_BADHOLE_STOF	Badhole flag from the Neutron stand-off
FMI	Fullbore Formation Microimager
g/cm ³	Gram per cubic centimetre
GAPI	Unit of radioactivity used for natural Gamma Ray logs
GEOLOG	Emerson software used for logs interpretation
GPCI	Geneva Petroleum Consultants International
GPIT	General Purpose Inclinometry Tool
GR	Total Gamma Ray
GR_KCOR	Total Gamma Ray corrected for mud potassium
GR_KCOR_PRED	GR_KCOR prediction by MultiMin
HAEMATITE	Haematite weight percentage from MultiMin

HALITE	Halite weight percentage from MultiMin
HDAR	Hole diameter from area
HDRA	Bulk density correction
HFK	Potassium concentration from HNGS
HI	Hydrogen Index
HNGS	Hostile Natural Gamma Ray Sonde
HRLT	High Resolution Laterolog array Tool
HSGR	HNGS Standard Gamma Ray
HTHO	Thorium concentration from HNGS
HURA	Uranium concentration from HNGS
HURA_PRED	HURA prediction by MultiMin
ILLITE	Illite weight percentage from MultiMin
KAOLIN	Kaolinite weight percentage from MultiMin
KEROGEN	Kerogen weight percentage from MultiMin
LEH.QT	Logging Equipment Head with Tension
LQC_INDEX	Log Quality Control Index
MCFL	Micro-Cylindrical Focused Log
MHF	Micro Hydraulic Fracturing
MSCL	Multi-sensor Core Logger
MULT_QC	MultiMin analysis quality flag
MULTIMIN	Multi mineral and multi fluid analysis module in Geolog software
m MD	Metre Measured Depth
MSIP	Modular Sonic Imaging Platform
NFUN	Number of MultiMin iterations
NO_K_CLAYS	Not potassic clays weight percentage from MultiMin
ORTHOCL	K-feldspars weight percentage from MultiMin
p.u.	Porosity unit
PEFZ	Photoelectric factor
PEFZ_PRED	PEFZ prediction by MultiMin
PHI_PICNO	Core pycnometer porosity
PHI_WL1	Core water-loss porosity (105 °C) using bulk wet density
PHI_WL2	Core water-loss porosity (105 °C) using grain density
PHIE	Effective porosity
PHIT	Total porosity

PLAGIO	Plagioclases weight percentage from MultiMin
PPC	Power Positioning device and Caliper tool
PRECALC	Precalculation module in the Geolog software
PYRITE	Pyrite weight percentage from MultiMin
QC	Quality Control
QF_SILICATES	Matrix quartz and feldspars weight percentage from MultiMin
QUALITY	MultiMin analysis quality
QUARTZ	Quartz weight percentage from MultiMin
RCL	Reduced Composite Log
RHGE_WALK2	Matrix density from elemental concentrations (WALK2 model)
RHOB_CALC	Bulk density computed from core data
RHOG	Grain density from MultiMin
RHOS	Solid density
RHOZ	Bulk density
RHOZ_PRED	RHOZ prediction by MultiMin
RT_HRLT	HRLT true formation resistivity
RUGO	Borehole wall rugosity
RXOZ	Invaded formation resistivity filtered at 18 inches
SIDER	Siderite weight percentage from multimin
SIGF	Macroscopic cross section for the absorption of thermal neutrons, or capture cross section, of a volume of matter, measured in capture units [c.u.]
SIGF_PRED	SIGF prediction by MultiMin
SLB	Abbreviation for Schlumberger Logging Company
SP	Spontaneous Potential
STOF	APS Stand-Off
SWE	Effective water saturation
SWT	Total water saturation
TLD	Three-detector Lithology Density
TOC	Total organic carbon [w/w or wt.-%]
U	Photoelectric cross-section computed by Precalc [b/cc]
UBI	Ultrasonic Borehole Imager
v/v	Volume per volume
VCL	Volume of wet clay

VOL_ANHYDR	MultiMin volume of anhydrite
VOL_ANORTH	MultiMin volume of plagioclase
VOL_CALCITE	MultiMin volume of calcite
VOL_CHLOR	MultiMin volume of chlorites
VOL_DOLOM	MultiMin volume of dolomite
VOL_ILLITE	MultiMin volume of illite
VOL_ORTHOCL	MultiMin volume of potassic feldspars
VOL_SIDER	MultiMin volume of siderite
VP	Compressional waves velocity [m/s]
VS	Shear waves velocity [m/s]
VPVS	Compressional and shear waves velocity ratio
VPVS_INPUT	Array Monte-Carlo input for VP/VS
W/W	Weight per weight
WANH_WALK2	Dry weight fraction anhydrite/gypsum from ECS (WALK2 model)
WCAR_WALK2	Dry weight fraction carbonate from ECS (WALK2 model)
WCLA_WALK2	Dry weight fraction clay from ECS (WALK2 model)
WEVA_WALK2	Dry weight fraction salt from ECS (WALK2 model)
WPYR_WALK2	Dry weight fraction pyrite from ECS (WALK2 model)
WQFM_WALK2	Dry weight fraction quartz+feldspar+mica from ECS (WALK2 model)
WSID_WALK2	Dry weight fraction siderite from ECS (WALK2 model)
XRD	X-Ray Diffraction
μs/ft	Microsecond per foot (unit for sonic slowness)

1 Introduction

1.1 Context

To provide input for site selection and the safety case for deep geological repositories for radioactive waste, Nagra has drilled a series of deep boreholes ("Tiefbohrungen", TBO) in Northern Switzerland. The aim of the drilling campaign is to characterise the deep underground of the three remaining siting regions located at the edge of the Northern Alpine Molasse Basin (Fig. 1-1).

In this report, we present the results from the Marthalen-1-1 borehole.

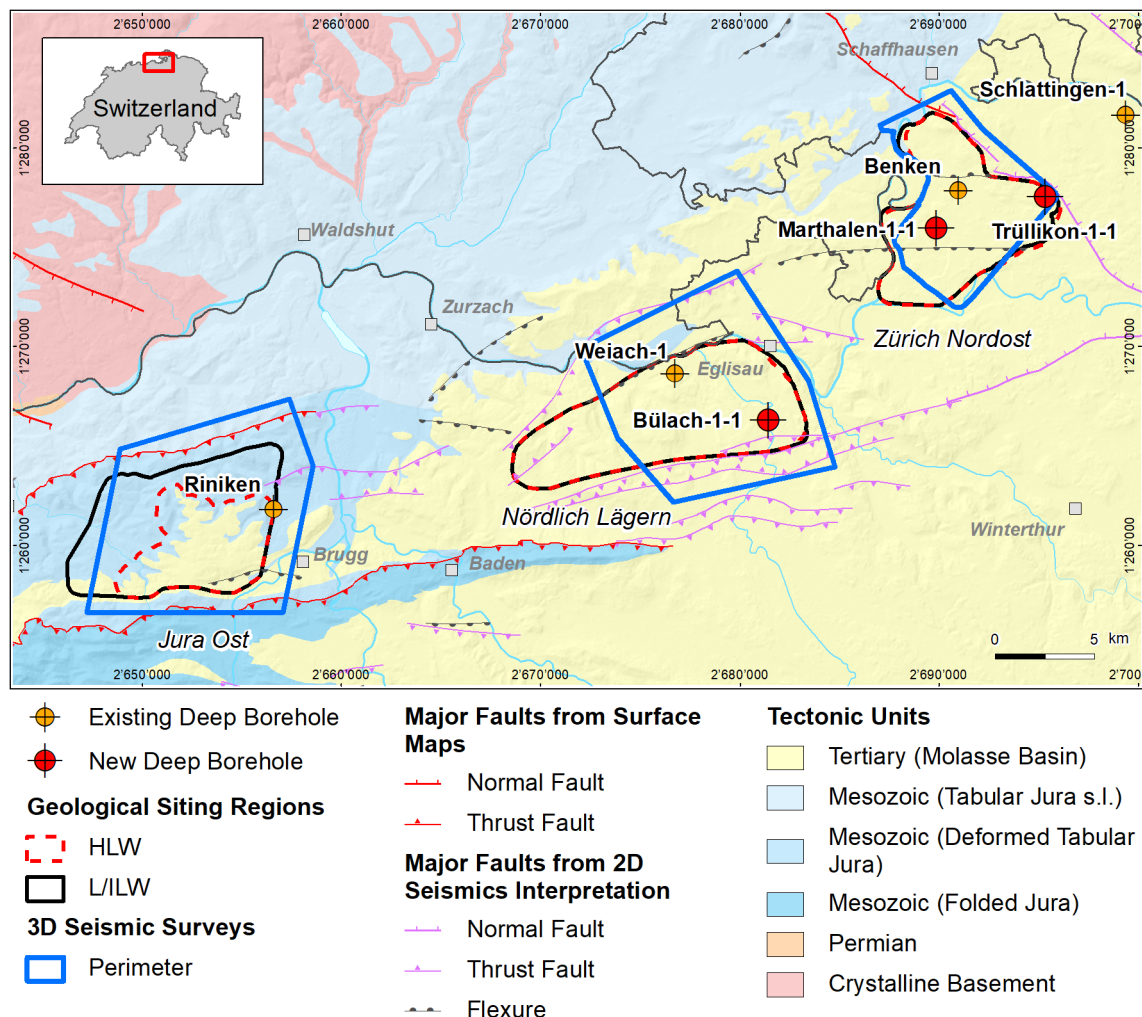


Fig. 1-1: Tectonic overview map with the three siting regions under investigation

1.2 Location and specifications of the borehole

The Marthalen-1-1 (MAR1-1) exploratory borehole is the third borehole drilled within the framework of the TBO project. The drill site is located in the western part of the Zürich Nordost siting region (Fig. 1-2). The vertical borehole reached a final depth of 1'099.25 m (MD)¹. The borehole specifications are provided in Tab. 1-1.

Tab. 1-1: General information about the MAR1-1 borehole

Siting region	Zürich Nordost
Municipality	Marthalen (Canton Zürich / ZH), Switzerland
Drill site	Marthalen-1 (MAR1)
Borehole	Marthalen-1-1 (MAR1-1)
Coordinates	LV95: 2'689'889.946 / 1'275'956.932
Elevation	Ground level = top of rig cellar: 399.48 m above sea level (asl)
Borehole depth	1'099.25 m measured depth (MD) below ground level (bgl)
Drilling period	9th February 2020 – 14th July 2020 (spud date to end of rig release)
Drilling company	Daldrup & Söhne AG
Drilling rig	Wirth B 152t
Drilling fluid	Water-based mud with various amounts of different components such as ² : 55 – 460 m: Bentonite & polymers 460 – 881 m: Potassium silicate & polymers 881 – 961 m: Sodium silicate & polymers 961 – 1'099.25 m: Sodium chloride & polymers

The lithostratigraphic profile and the casing scheme are shown in Fig. 1-3. The comparison of the core versus log depth³ of the main lithostratigraphic boundaries in the MAR1-1 borehole is shown in Tab. 1-2.

¹ Measured depth (MD) refers to the position along the borehole trajectory, starting at ground level, which for this borehole is the top of the rig cellar. For a perfectly vertical borehole, MD below ground level (bgl) and true vertical depth (TVD) are the same. In all Dossiers depth refers to MD unless stated otherwise.

² For detailed information see Dossier I.

³ Core depth refers to the depth marked on the drill cores. Log depth results from the depth observed during geophysical wireline logging. Note that the petrophysical logs have not been shifted to core depth, hence log depth differs from core depth.

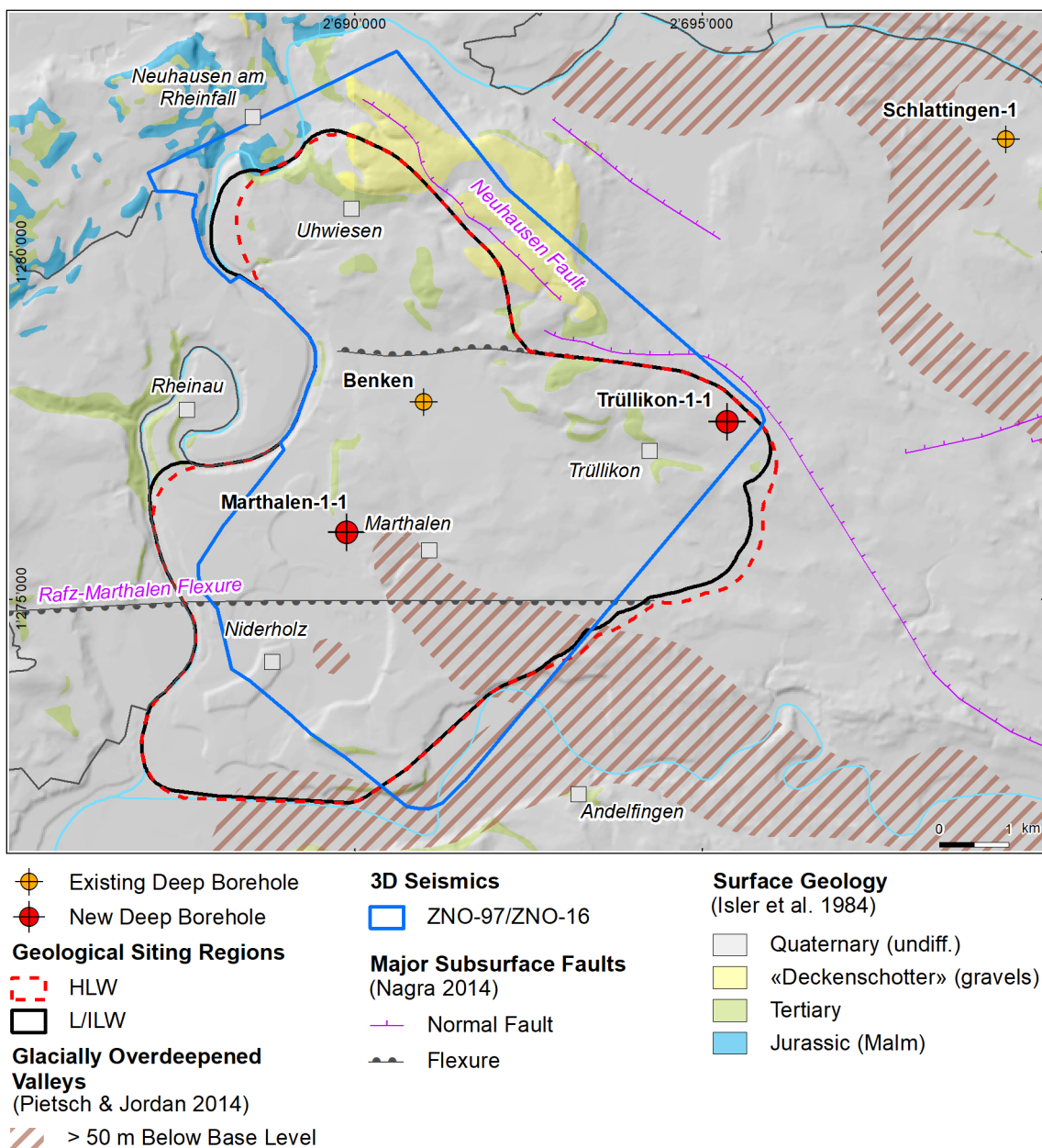
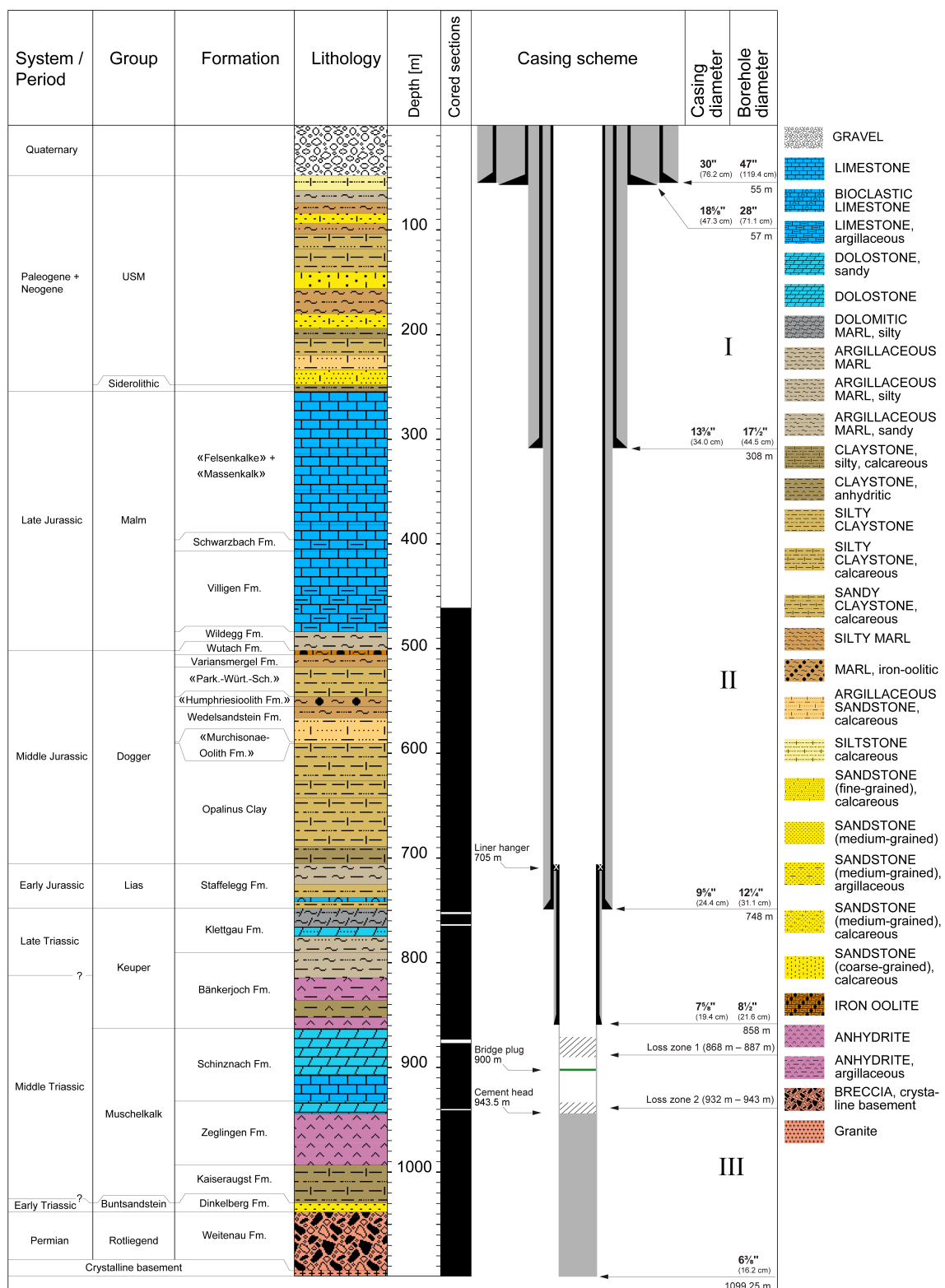


Fig. 1-2: Overview map of the investigation area in the Zürich Nordost siting region with the location of the MAR1-1 borehole in relation to the boreholes Benken, Schlattingen-1 and TRU1-1

Fig. 1-3: Lithostratigraphic profile and casing scheme for the MAR1-1 borehole⁴⁴ For detailed information see Dossier I and III.

Tab. 1-2: Core and log depth for the main lithostratigraphic boundaries in the MAR1-1 bore-hole⁵

System / Period	Group	Formation	Core depth in m	Log (MD)
Quaternary				48
Paleogene + Neogene	USM		248	—
	Siderolithic			254
		«Felsenkalke» + «Massenkalk»		396.1
	Malm	Schwarzbach Formation		406.9
		Villigen Formation	484.02	484.22
		Wildegg Formation	501.80	501.92
		Wutach Formation	505.75	506.03
Jurassic		Variansmergel Formation	517.43	517.57
		«Parkinsoni-Württembergica-Schichten»	545.93	546.12
	Dogger	«Humphriesioolith Formation»	555.23	555.47
		Wedelsandstein Formation	589.17	589.19
		«Murchisonae-Oolith Formation»	590.35	590.37
		Opalinus Clay	705.40	705.52
	Lias	Staffelegg Formation	747.83	747.89
	Keuper	Klettgau Formation	790.12	790.34
		Bänkerjoch Formation	862.52	862.77
Triassic		Schinznach Formation	932.24	932.47
	Muschelkalk	Zeglingen Formation	993.50	993.97
		Kaiseraugst Formation	1029.45	1029.95
	Buntsandstein	Dinkelberg Formation	1037.98	1038.23
Permian	Rotliegend	Weitenau Formation	1094.08	1094.08
		Crystalline Basement	1099.25	final depth

⁵ For details regarding lithostratigraphic boundaries see Dossier III and IV; for details about depth shifts (core gonio-metry) see Dossier V.

1.3 Documentation structure for the MAR1-1 borehole

NAB 21-20 documents the majority of the investigations carried out in the MAR1-1 borehole, including laboratory investigations on core material. The NAB comprises a series of stand-alone dossiers addressing individual topics and a final dossier with a summary composite plot (Tab. 1-3).

This documentation aims at early publication of the data collected in the MAR1-1 borehole. It includes most of the data available approximately one year after completion of the borehole. Some analyses are still ongoing (e.g. diffusion experiments, analysis of veins, hydrochemical interpretation of water samples) and results will be published in separate reports.

The current borehole report will provide an important basis for the integration of datasets from different boreholes. The integration and interpretation of the results in the wider geological context will be documented later in separate geoscientific reports.

Tab. 1-3: List of dossiers included in NAB 21-20

Black indicates the dossier at hand.

Dossier	Title	Authors
I	TBO Marthalen-1-1: Drilling	P. Hinterholzer-Reisegger & B. Garitte
II	TBO Marthalen-1-1: Core Photography	D. Kaehr & M. Gysi
III	TBO Marthalen-1-1: Lithostratigraphy	P. Jordan, P. Schürch, H. Naef, M. Schwarz, R. Felber, T. Ibele & M. Gysi
IV	TBO Marthalen-1-1: Microfacies, Bio- and Chemostratigraphic Analyses	S. Wohlwend, H.R. Bläsi, S. Feist-Burkhardt, B. Hostettler, U. Menkveld-Gfeller, V. Dietze & G. Deplazes
V	TBO Marthalen-1-1: Structural Geology	A. Ebert, L. Gregorczyk, E. Hägerstedt, S. Cioldi & M. Gysi
VI	TBO Marthalen-1-1: Wireline Logging and Micro-hydraulic Fracturing	J. Gonus, E. Bailey, J. Desroches & R. Garrard
VII	TBO Marthalen-1-1: Hydraulic Packer Testing	R. Schwarz, S.M.L. Hardie, H.R. Müller, S. Köhler & A. Pechstein
VIII	TBO Marthalen-1-1: Rock Properties, Porewater Characterisation and Natural Tracer Profiles	U. Mäder, L. Aschwanden, L. Camesi, T. Gimmi, A. Jenni, M. Kiczka, M. Mazurek, D. Rufer, H.N. Waber, P. Wersin, C. Zwahlen & D. Traber
IX	TBO Marthalen-1-1: Rock-mechanical and Geomechanical Laboratory Testing	E. Crisci, L. Laloui & S. Giger
X	TBO Marthalen-1-1: Petrophysical Log Analysis	S. Marnat & J.K. Becker
	TBO Marthalen-1-1: Summary Plot	Nagra

1.4 Scope and objectives of this dossier

The dossier at hand describes the results of the stochastic petrophysical log analysis performed in the MAR1-1 borehole. The detailed workflow for this analysis is described in a methodology report (Marnat & Becker 2021, NAB 20-30). Here, only a very short summary is given. The lowest vertical resolution tools, such as ECS, Gamma Ray or Sonic, are limiting the resolution of the MultiMin analysis. High resolution and standard tools cannot be mixed in a same processing. For this reason, only the standard resolution version of the logs was input with a sampling rate of $\frac{1}{2}$ foot (~ 15 cm).

For the Multimineral Log Analysis (abbreviation MultiMin throughout this report), a mineral content is assumed at each of these measurement locations, either from prior knowledge or from mineralogical lab analyses. A theoretical log response from this assumed mineral content for each available petrophysical log is calculated and compared to the measured log. Using optimisation techniques, the difference (i.e. the error) between calculated log responses and measured petrophysical logs is minimised by adjusting the assumed mineral content. Any deviation from this workflow is explained in this report.

The result of this analysis, therefore, are continuous profiles of the mineralogical content and other rock parameters (e.g. porosity) where the main aim of these calculations here were continuous profiles of the clay content and porosity.

The organisation of this dossier follows the necessary steps of the workflow. First, data is collected, and quality checks (QC) are performed. In addition, necessary pre-calculations concerning important environmental parameters are performed (Chapter 2). This is followed by the actual analysis of the data (Chapter 3) and a short description of results in Chapter 4. Chapter 4 also includes an estimation of the fit of the results to available data from lab measurements.

All depths in this report are reported as measured depths from top rig cellar (MD) if not stated otherwise.

2 Data preparation

2.1 Used log data

The acquisition, QC (quality control) and generation of log composites of the petrophysical logs from the MAR1-1 borehole is described in more detail in Dossier VI, the raw corrected log data is also shown in Plate 1. Note that abbreviations in brackets in the list below are according to Schlumberger (SLB) mnemonics (as SLB was the log contractor responsible for the log acquisition). A detailed description of how the different tools measure the respective parameters and the underlying physics behind these measurements is not the focus of this report and can be found in Dossier VI, Chapter 3.1. The petrophysical logs used for this study are listed below:

- **Caliper log** (EMS/PPC – Environmental Measurement Sonde/Powered Positioning Caliper). The caliper log uses several coupled pairs of mechanical arms (2 pairs with PPC, 3 pairs with EMS) to continuously measure the borehole shape in different orientations.
- **Gamma Ray** (GR, from the EDTC – Enhanced Digital Telemetry Cartridge). This log measures the total naturally occurring radioactivity which can be used to determine the mineral content (mainly clay).
- **Spectral Gamma Ray** (SGR, from the HNGS – Hostile Natural Gamma Ray Sonde). This tool also measures the naturally occurring radioactivity. In addition to the total radioactivity, the tool is able to determine the amount (in ppm or wt.-%) of uranium (U), thorium (Th) and potassium (K) in the rocks which can be used e.g. for clay typing.
- **Neutron Hydrogen Index** (APLC curve, from APS – Accelerator Porosity Sonde). The APS is a tool that can measure the neutron hydrogen index in water saturated formations. This measurement is corrected for an environmental effect and normalised to limestone matrix. SLB refers to this corrected curve as APLC (Near/Array Corrected Limestone Porosity). In addition, the APS can be used to determine **Sigma** (SIGF), a measure to determine the water content and mineralogical characterisations.
- **Density** (TLD – Three-detector Lithology Density). TLD is an induced radiation tool that measures the bulk density of the formation and the photoelectric factor (PEF). It uses a radioactive source to emit gamma photons into the formation. The gamma rays undergo Compton scattering by interacting with the atomic electrons in the formation. Compton scattering reduces the energy of the gamma rays in a stepwise manner and scatters the gamma rays in all directions. When the energy of the gamma rays is less than 0.5 MeV, they can undergo photoelectric absorption by interacting with the electrons. The flux of gamma rays that reach each of the detectors of the TLD is therefore attenuated by the formation, and the amount of attenuation is dependent upon the electronic density of the formation, which is related to its bulk density. In addition, the TLD provides the **photoelectric absorption index** (photoelectric factor – PEF), which represents the probability that a gamma photon will be photoelectrically absorbed per electron of the atoms that compose the material. The PEF characterises the mineralogy. The TLD tool is housed in the High-Resolution Mechanical Sonde that also includes the Micro-Cylindrically Focused Log (MCFL) sonde, that measures the microresistivity or alternatively, the resistivity very close to the borehole wall (RXOZ).
- **Element Spectroscopy** (ECS – Elemental Capture Spectroscopy). The ECS is also an induced radiation tool with a radioactive neutron source. The ECS measures the concentration of a series of elements in the formation by analysing the spectrum of back scattered gamma rays. The following elements are used in this report: DWSI_WALK2 (Si), DWCA_WALK2 (Ca), DWFE_WALK2 (Fe), DWSU_WALK2 (S), DWTI_WALK2 (Ti). Special processing techniques allow under certain circumstances the measurement of supplementary elements

such as Mg (MGWALK closure model, DWMG_MGWALK curve); Al, K and Na (ALKNA closure model, with ALKNA suffix). The element spectroscopy measurements are provided in percent.

During the QC process of the ECS acquisition, the DWMG_MGWALK response could be validated in the pure dolostones, reading close from the theoretical endpoint for dolostones: 0.132 W/W.

The iron concentration from the ECS WALK2 model was found systematically overestimating the XRF measurements on core samples. A correction was performed founded on the ECS and XRF results in MAR1-1. The resulting iron concentration curve was called DWFE_CORR.

- **Resistivity** (HRLT – High Resolution Laterolog array Tool). The HRLT measures the formation electrical resistivities at different depths of investigation, providing a mud filtrate invasion profile, if any invasion. Processing allows the extrapolation of the resistivity measurements far into the formation (true formation resistivity), as well as close to the borehole wall (microresistivity). The resistivity is a function of the water content of the formation and its salinity.
- **Sonic** (MSIP – Modular Sonic Imaging Platform). The MSIP measures the formation interval transit time, a measure of how fast seismic waves (compressional, shear and Stoneley waves) propagate through the formation.

An overview of the used petrophysical logs and their measurements in the MAR1-1 borehole is given in Plate 1.

Usable log data were available for analysis from 312.3 to 1'077.47 m. Due to gaps between drilling sections and cased hole sections (see borehole report, Dossier VI), a minor MultiMin interpretation gap, due to insufficient petrophysical logs coverage, remained in the following interval, as shown in Fig. 2-1:

- 750.0 – 752.5 m (Run 3.2.X, 9 $\frac{5}{8}$ " casing at 746 m MD Driller)

In the upper interval (0 – 309 m Driller's depth), only technical logging was performed which is not suitable for the log interpretation routines used here (only gamma ray and cement evaluation, 0 – 309 m are available; see Dossier VI). However, this interval is only of minor interest in terms of formation characterisation for the geological disposal of radioactive waste and, hence, was disregarded completely.

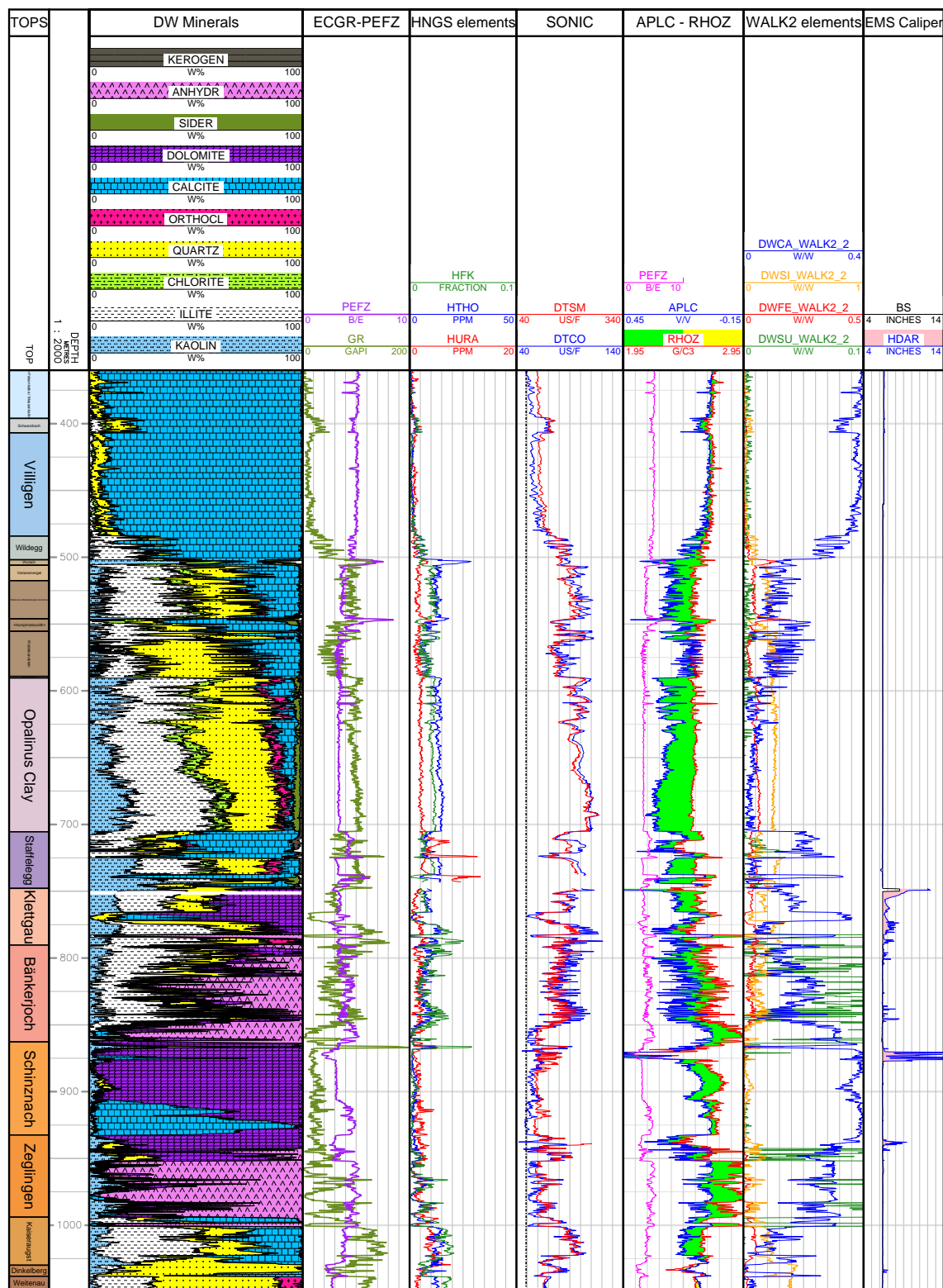


Fig. 2-1: Petrophysical log availability and gaps in the borehole MAR1-1

Please note that ECS elements are displayed as measured (in weight/weight, 0 – 1 w/w range) and are not converted to wt.-% (weight percentage) here.

2.2 Used core data

As previously mentioned, the MultiMin algorithm requires an initial assumption of the mineralogical content. For calibration of the log interpretation, core data (lab measurements of mineralogy, total porosity and density) were used (see Dossier VIII for more details on core data, some core data is shown in Plate 2). 124 core samples collected at depths ranging from 464.92 to 1'053.55 m were available of which 78 were analysed for pycnometer total porosity, 101 for water loss total porosity, 94 for XRD mineralogy and 29 for clay types. The analysed minerals were quartz, K-feldspars, plagioclase, calcite, dolomite/ankerite, siderite, anhydrite, celestite, pyrite, clay minerals and organic carbon. The 29 samples analysed for clay typing (in the interval 638.20 – 1'026.55 m) quantified the illite, smectite, kaolinite and chlorite endmembers. The mineral content was used to calibrate the MultiMin interpretation.

As mentioned earlier, porosities and grain densities are also included in the core data and hence used for this study. The three measured porosities (water-loss porosity (105 °C) using bulk wet density, water-loss porosity (105 °C) using grain density and pycnometer porosity) were accounted for, the most relevant was selected compared to the MultiMin total porosity ($\text{PHIT } \Phi_t$). The relative errors of these measurements are provided as well. For more details on the exact measurement procedures of these parameters see Waber (ed.) (2020).

The difference between core and log depth has been reported in Dossier V. As the reported depth differences are much smaller than the wireline logs vertical resolution, it was decided not to apply the shift to the core data in this study.

2.3 Multi-sensor Core Logger (MSCL) data

MSCL measurements from cores were available for parts of the MAR1-1 borehole (from 499.00 to 792.88 m). Measurements were performed in the interval of the host rock (Opalinus Clay) and its confining units. The following parameters were measured:

- Bulk density in g/cc
- Compressional (P) wave velocity in m/s
- Spectral gamma ray curves: potassium (K, %), thorium (Th, ppm) and uranium (U, ppm)
- XRF (X-ray fluorescence) elemental analysis: iron (Fe), silicon (Si), calcium (Ca), aluminium (Al), titanium (Ti) and sulphur (S) are used for this study.

Some ECS data could not be acquired between drilling sections, leaving a gap. In this same interval, no XRF data is available to fill the gaps.

The XRF elemental analysis results were compared with the same element concentrations from the ECS logging (WALK2 closure model). The MSCL data (also referred to as core logs in this report) covers the measured interval at variable sampling rates (usually 0.05 m).

This comparison is shown in Fig. 2-2, the core logs were not depth-shifted.

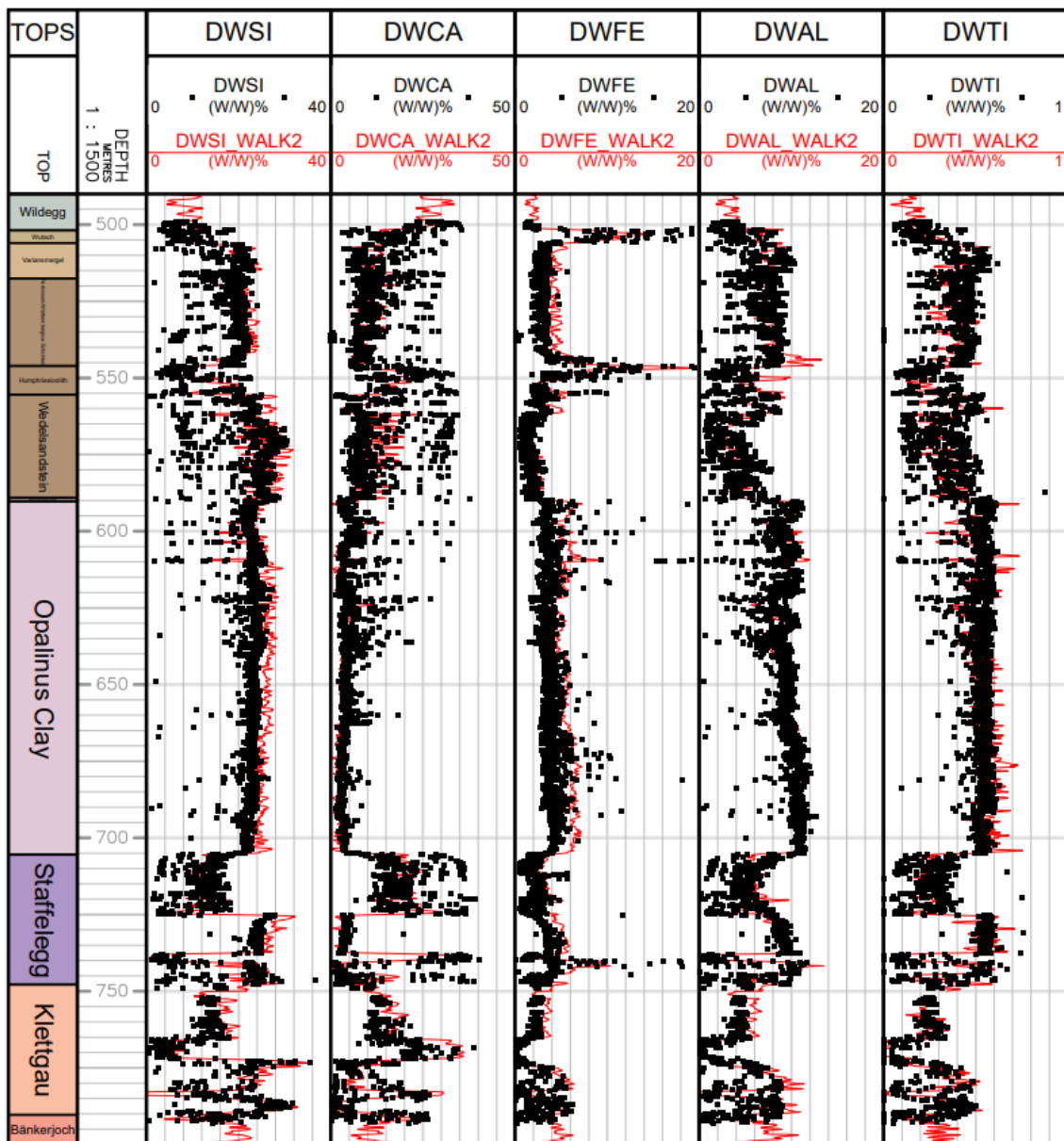


Fig. 2-2: XRF (black dots) and ECS WALK2 (red curves) elements comparison

While the calcium, aluminium and titanium concentrations are almost similar, the XRF iron and silicon are lower than from the ECS WALK2 closure model.

A correlation was used to correct the ECS iron content to XRF, with the following equation:

$$\text{DWFE_CORR} = 0.0375 + 0.396 * \text{DWFE_WALK2} + 4.882 * \text{DWFE_WALK2}^2$$

The same check was done for the core and HNGS spectral gamma ray (see Fig. 2-3).

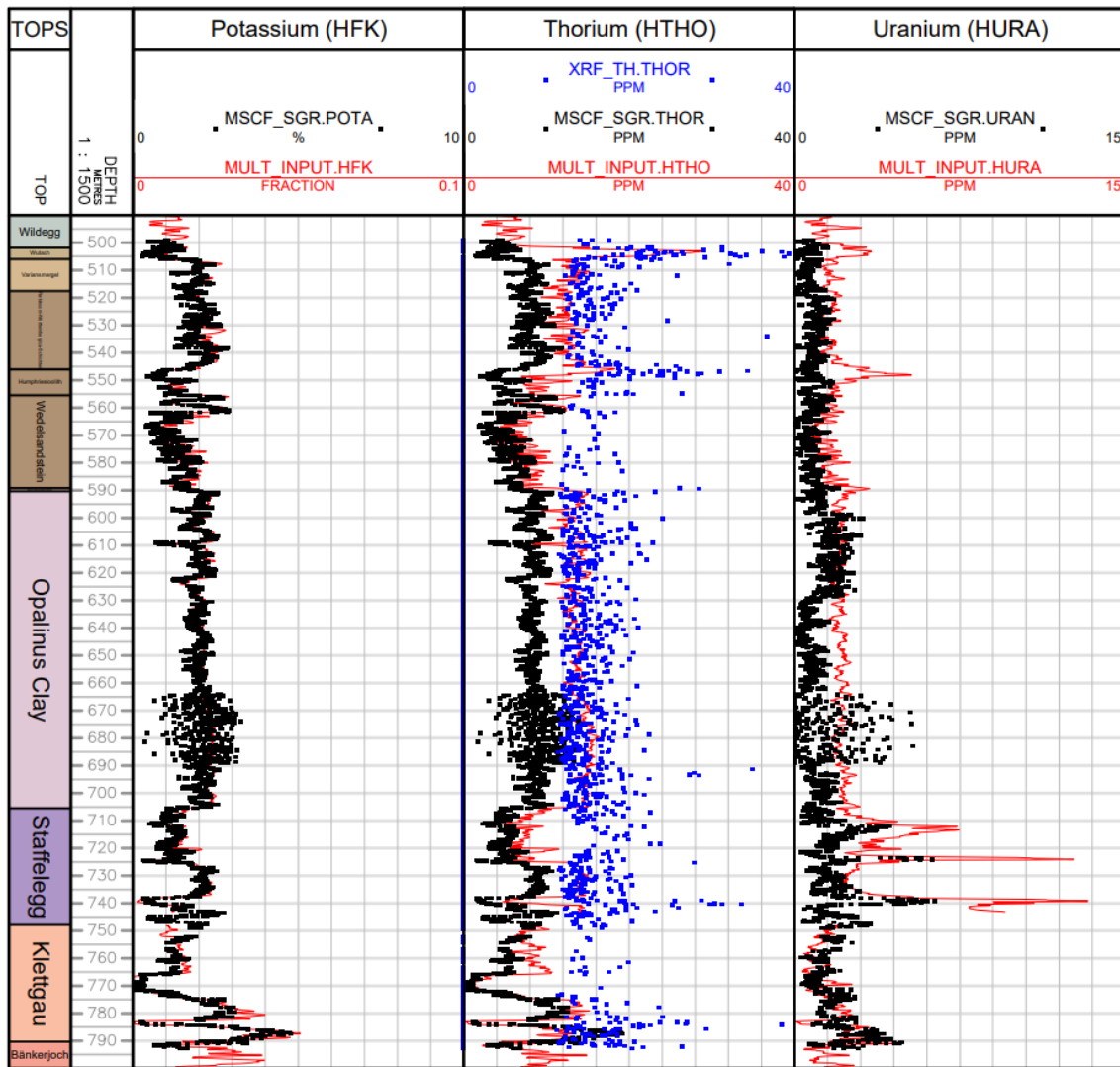


Fig. 2-3: Core (black dots: Spectral Gamma Ray, blue dots: XRF thorium) and wireline HNGS (red curves) Spectral Gamma Ray elements comparison

Uranium from the XRF scanner was not measured because it was below the detection limit of the scanner.

The potassium from MSCL is almost similar to HFK from HNGS. The MSCL uranium is close but locally inconsistent with HURA. The uranium from XRF was not reported because it was below the detection limit of the used XRF scanner.

The HTHO from HNGS is often much higher than the thorium content measured with the MSCL. The XRF thorium (blue dots) is not usable, showing too much dispersion. Hence, the MSCL data was used indirectly for a QC and subsequently to correct petrophysical log measurements, namely the iron content of the ECS measurements.

2.4 MultiMin input dataset preparation

The petrophysical composite log used as input for this study (see Dossier VI) represents a quality controlled, edited, corrected and merged dataset for a selection of the most important petrophysical logging data recorded in each section of the borehole. As mentioned earlier, a gap in the coverage of the borehole with the petrophysical logs occurs. The original measurements and corrections of the petrophysical logs are reported in Dossier VI.

The only deviation to this source dataset is the use of the corrected DWFE_CORR.

2.5 Preliminary calculations (Precalc)

As the wireline logs measure parameters under in situ conditions (e.g. temperatures depending on depth and temperature of the borehole fluid, infiltration of mud into the formation depending on the borehole fluid and its density etc.), these prevailing conditions in the borehole have to be taken into account to correctly predict/calculate the theoretical log response from the assumed mineral and fluid content (i.e. total porosity) at a certain depth. Continuous profiles of these environmental parameters were calculated using the Precalc module from the interpretation software Geolog. The main parameters used for the calculation of these environmental parameters are, for reasons of transparency and to be able to replicate exactly the analyses reported here, displayed in Appendix 1.

The mud properties (mud density and resistivities) reported here were extracted from the validated SLB wireline log headers (see Dossier VI).

3 Petrophysical log interpretation

3.1 MultiMin interpretation

In the following, the petrophysical log interpretation and its results are shortly described. All necessary data treatment and environmental pre-calculations have been described in the previous chapters or are described in the Methodology report (Marnat & Becker 2021, NAB 20-30). Many qualitatively good wireline logs were available in most sections of the borehole, allowing the computation of many unknowns (fluids and minerals).

Significant hydrocarbon shows were neither described by the mudlogging nor inferred from cores or petrophysical logs. Consequently, the formations were treated as water wet (i.e. with saline water as the pore fluid).

The main minerals were inferred from the XRD measurements on core samples and regional knowledge (XRD data from previously drilled boreholes Bülach1-1 and Trüllikon-1 (*cf.* Dossiers VIII of the respective borehole reports), Weiach-1 and Benken-1 from Mazurek 2017). Using the MultiMin approach, the mineral content for the following minerals were modelled:

- Clay mineral endmembers (kaolinite, illite, smectite and chlorites) and total clay mineral content. From the available wireline logs, smectite cannot be differentiated from kaolinite.
- Silicates: quartz, potassic feldspars, plagioclases
- Carbonates: calcite, siderite, dolomite/ankerite; iron oxide, to honour the ECS iron content in the formations just above the Opalinus Clay, as the measured siderite, pyrite and chlorite only cannot explain the DWFE_CORR values. Note that the problem would be even worse with the raw DWFE_WALK2 curve.
- Evaporites: anhydrite
- Organic carbon (kerogen)

These compounds were modelled depending on the available data. In case not enough data were available for a given interval (e.g. where data was missing or of insufficient quality), some minerals were merged to a pseudo-mineral to reduce the number of unknowns (see Marnat & Becker 2021 for more details).

Tab. 3-1 shows an example of the interpretation intervals, the available data and the MultiMin model names used in each interval. The intervals are defined based on their consistent mineralogy, available logs and consistent environmental parameters (e.g. mud system changes). Interpretation intervals may be subdivided further, e.g. to respect a reduced data quality. The full table with all intervals is available in Appendix B.

Tab. 3-1: List of MultiMin models used in MAR1-1

The intervals (column Interval Name) may include several MultiMin models if some of the input data were of bad quality or the particular section of the interval required special assumptions due to its assumed mineralogy.

The column Cond Num stands for model condition number. Low values are typical for good mathematical models (below 4.00). Condition numbers above 4.00 highlighted in yellow correspond to fair models. See Section 3.2 for more information.

From [m]	To [m]	Interval name	Multimin Models	Cond. Number	Description
309.0	334.0	INT1	mar11_int1	3.08	Malm, good hole
334.0	349.0	INT1	mar11_int1_bh	3.47	Malm, bad hole
349.0	405.0	INT1	mar11_int1	3.08	Malm, good hole
405.0	407.0	INT1	mar11_int1_bh	3.47	Bad hole
407.0	484.0	INT1	mar11_int1	3.08	Malm, good hole
484.0	502.0	INT2_top	mar11_int2_top	4.89	Wildegg Fm., «Brauner Dogger»
502.0	505.0	INT2_top	mar11_int2_wut	4.55	Wutach Fm.
505.0	590.5	INT2_top	mar11_int2_top	4.89	Wildegg Fm., «Brauner Dogger»
590.5	725.0	INT2	mar11_int2_opa	3.93	Opalinus Clay
725.0	737.0	INT2_base	mar11_int2_base	3.86	Staffelegg Fm.
737.0	743.0	INT2_base	mar11_int2_bot1	3.77	Reduced dataset
743.0	748.0	INT2_base	mar11_int2_bot2	3.39	Reduced dataset
748.0	750.0	INT3	mar11_int3_top	4.27	Unreliable density-neutron
752.0	854.7	INT3	mar11_int3	3.11	Klettgau & Bänkerjoch Fm.
854.7	867.5	INT4	mar11_int4	3.35	
867.5	870.8	INT4	mar11_int4_bh	2.76	Bad hole
870.8	871.8	INT4	mar11_int4_bh1	2.76	Bad hole
871.8	876.0	INT4	mar11_int4_bh	2.76	Bad hole
876.0	937.0	INT4	mar11_int4	3.35	
937.0	939.0	INT4	mar11_int4_no_dts	3.35	Missing DTS curve
939.0	994.0	INT4	mar11_int4	3.35	
994.0	1'030.0	INT5	mar11_int5	2.45	Kaiseraugst Fm.
1'030.0	1'038.0	INT6	mar11_int6	4.26	Dinkelberg Fm.
1'038.0	1'049.0	INT7	mar11_int7	4.46	Weitenau Fm.
1'049.0	1'077.3	INT7_base	mar11_int7base	2.24	Weitenau Fm., no APS, no ECS

Given the complexity of the MultiMin models applied to the MAR1-1 wireline logging data, an inverse linear modelling of the MultiMin endpoints could not be attempted in MAR1-1. Therefore, mineral and fluid endpoints were manually optimised to both reduce the difference between measured and predicted logs and match the core mineralogy and porosity. Greatly simplified, an

endpoint can be regarded as a factor that is used to calculate the theoretical log response for each mineral (e.g. if it is assumed that the endpoint for the density of calcite is 2.71 g/cc, a mineral content of 100% calcite should result in a density of 2.71 g/cc of the predicted density log. For a detailed explanation see Marnat & Becker (2021).

Based on expert judgement, an uncertainty value for the petrophysical logs was estimated and used to adjust the weight given to the respective log in the MultiMin computation. Again, greatly simplified, if the uncertainty values are large, the corresponding log response will be predicted in the MultiMin interpretation, but it will not be used in the process of error minimisation and hence has no impact on the result of the MultiMin interpretation (for more details see Marnat & Becker 2021). High uncertainty values often apply to the Sonic curves, the PEFZ (as PEFZ is already used for the U computation, Photo-electric cross-section) and the electrical conductivities.

The detailed parameters for all the MultiMin models are available in tables in Appendix 3.

3.2 Bad-hole treatment and quality of results

The quality of the MultiMin interpretation relies in part on the quality of the input data. However, it also relies on the number of available curves and the number of unknowns (i.e. minerals) that need to be calculated. Hence, several quality indicators exist that either are informative about the quality of the input data (LQC-Index), the definition of the mathematical model (CONDNUM, NFUN) or the quality of the interpretation results (MULT_QC and QUALITY).

3.2.1 Indicator for input data quality (LQC_INDEX)

During each wireline logging, the borehole shape is determined using a caliper log. If the borehole shape deteriorates far from the bit size (BS) and bit shape (usually circular), some (or all) of the wireline logs may measure biased data, because the distance between the log and the borehole wall is too large. In that case, the response of a considerable amount of borehole fluid is measured by the tool, and the measurements represent more the petrophysical parameters of the borehole fluid than of the formation.

Four bad-hole indicators, which can be used as a quality measure of the data, are calculated from some of the available wireline logs:

1. FLAG_BADHOLE_DN: Neutron-Density crossplot
2. FLAG_BADHOLE_OVERGAUGE: HDAR > 1.15 * Bit Size
3. FLAG_BADHOLE_RUGO: Borehole wall rugosity, HDRA > 0.025 g/cc: HDRA (bulk density correction) is a correction of the bulk density measured with a gamma-gamma type logging device (here TLD). If this correction factor is larger than 0.025 g/cc, the indicator is triggered.
4. FLAG_BADHOLE_STOF: APS Neutron standoff > 0.35 in

For detailed information about these four indicators, please refer to Dossier VI.

These four indicators have two possible values: 0 in good hole or 1 in bad hole. They were combined to generate a log quality control flag (LQC_INDEX) using the following equation:

$$\begin{aligned} \text{LQC_INDEX} = & (\text{FLAG_BADHOLE_DN} + \text{FLAG_BADHOLE_OVERGAUGE} + \\ & \text{FLAG_BADHOLE_RUGO} + \text{FLAG_BADHOLE_STOF}) / 4 \end{aligned}$$

Hence, the value of the LQC-Index must be between 0 and 1 (and can only have values of 0, 0.25, 0.5, 0.75 or 1).

3.2.2 Indicator for the mathematical model (CONDNUM and NFUN)

CONDNUM

The CONDNUM stands for model condition number. Low values are typical for good mathematical models (below 4.00). Condition numbers above 4.00 correspond to fair models. CONDNUM is shown in Plate 1. A list of CONDNUMs for the different MultiMin interpretation intervals is given in Tab. 3-1. Please note that CONDNUM is not a proxy for the quality of the calculated output but only for the definition of the mathematical model to calculate the said output.

NFUN

NFUN indicates how many iterations were required to fulfil the constraints imposed by the available data where fewer numbers of iterations are indicative for a more robust model. NFUN is also shown in Plate 1. Please note that NFUN, as CONDNUM, is not a proxy for the quality of the calculated output but only for the definition of the mathematical model to calculate the said output.

3.2.3 Indicator for the MultiMin interpretation results (MULT_QC and QUALITY)

MULT_QC

The MultiMin results were not edited in MAR1-1 (e.g. less reliable data were not removed from the interpretation results), but an integrative MultiMin QC flag was generated (MULT_QC) combining several of the aforementioned quality indicators to inform the data user of potentially invalid results. As this flag relies on the availability of lab measurements, it is only available where a respective lab measurement is available. The MULT_QC flag relies on expert judgement and can have values of 2, 1 or 0 based on the three different scenarios detailed below:

- Highly suspicious porosity spikes occur and usually are correlated to an LQC-Index above or equal to 0.5, the quality curve (displayed in Plates 1 and 2, see below) can show values above 2, and the MultiMin results do not match the core measurements: MULT_QC = 2. A value of 2 in MULT_QC corresponds to most likely unreliable data.
- Suspicious porosity spikes occur but with a usually acceptable LQC-Index (0 or 0.25) and MultiMin quality curve values below 2: MULT_QC = 1. This value indicates that results can/should be used for the characterisation of the formation but should be treated with caution as the interpreted results are not a perfect fit with the available data.
- Otherwise, MULT_QC = 0. Interpreted results are reliable and can be used to characterise the formation.

QUALITY

In addition, a quality curve is shown in Plates 1 and 2. This curve is an indication of how well the observed measurements from wireline logs and the predicted results are part of the same population. At a value of QUALITY less than one, the calculated accuracy is within 95% compared to the original wireline logs, and therefore the analysis is of good quality. If the value is consistently above one, log measurements are not well honoured by the predicted curves, hence the analysis must be regarded as less robust.

Please note that the quality curve only compares the results of the MultiMin interpretation with the petrophysical logs and does not take data quality of the petrophysical logs (e.g. in bad hole sections) or lab measurements into account. The only indicator combining information on input data quality and interpretation result is the MULT_QC indicator detailed above.

4 Results of the calibrated stochastic log interpretation

In the following, the main results of the stochastic log interpretation are summarised. Plate 1 shows the measured wireline logs together with the calculated output from the MultiMin approach. The main results in terms of mineral content and porosity are displayed in Plate 2 as continuous curves. Plate 2 also shows the available lab measurements (from core data).

The aim of this chapter is not a detailed description and characterisation of the sedimentary sequence based on log interpretation results, but rather gives a more general description of the data and a general characterisation of the stratigraphic system or groups shown in Plate 2. Section 4.1 compares the interpretation results with core data giving an overview on the robustness of the interpreted mineralogical content in the borehole. Section 4.2 gives a general characterisation while Section 4.3 gives a more detailed description of calculated parameters in the Opalinus Clay.

4.1 Comparison of interpretation results with core data

Below, the MultiMin interpretations are compared to the mineralogical (bulk) and petrophysical measurements (porosity).

Due to the log database constraints and the need for robust mathematical MultiMin models (i.e. condition numbers ideally below 5 for fair to good models), the number of modelled minerals had to be adjusted. For the sake of easy comparison, the minerals had to be grouped:

- Quartz and feldspars (plagioclase and orthoclase) are grouped into a single pseudo-mineral (called QF-silicates in Plate 2).
- Different clay minerals were computed when possible (kaolinite – smectite together, chlorites: not potassic clays, called NO_K_CLAYS, and illite). All clay minerals were added to a (total) clay content (DRY_CLAYS).
- Comparable to the clay minerals, different carbonate minerals were also calculated (calcite, dolomite and siderite). In Plate 2, a track displays the total amount of carbonates (called carbonates). Next to it, two tracks show the calcite and dolomite content, as the latter two can be used to distinguish between some formations, especially below the Opalinus Clay.

Figs. 4-1 to 4-6 show crossplots between mineral weight percentages from cores (X axis, from XRD lab analyses) and interpretation results from MultiMin (Y axis).

Fig. 4-7 shows the crossplot between total porosity from core (X axis, Water-loss porosity (105 °C) using grain density lab measurement) and interpretation results from MultiMin (Y axis).

All available data are displayed together, covering the interval from the Villigen to the Weitenau Formations. The color coding represents the formations, as per the attached legend.

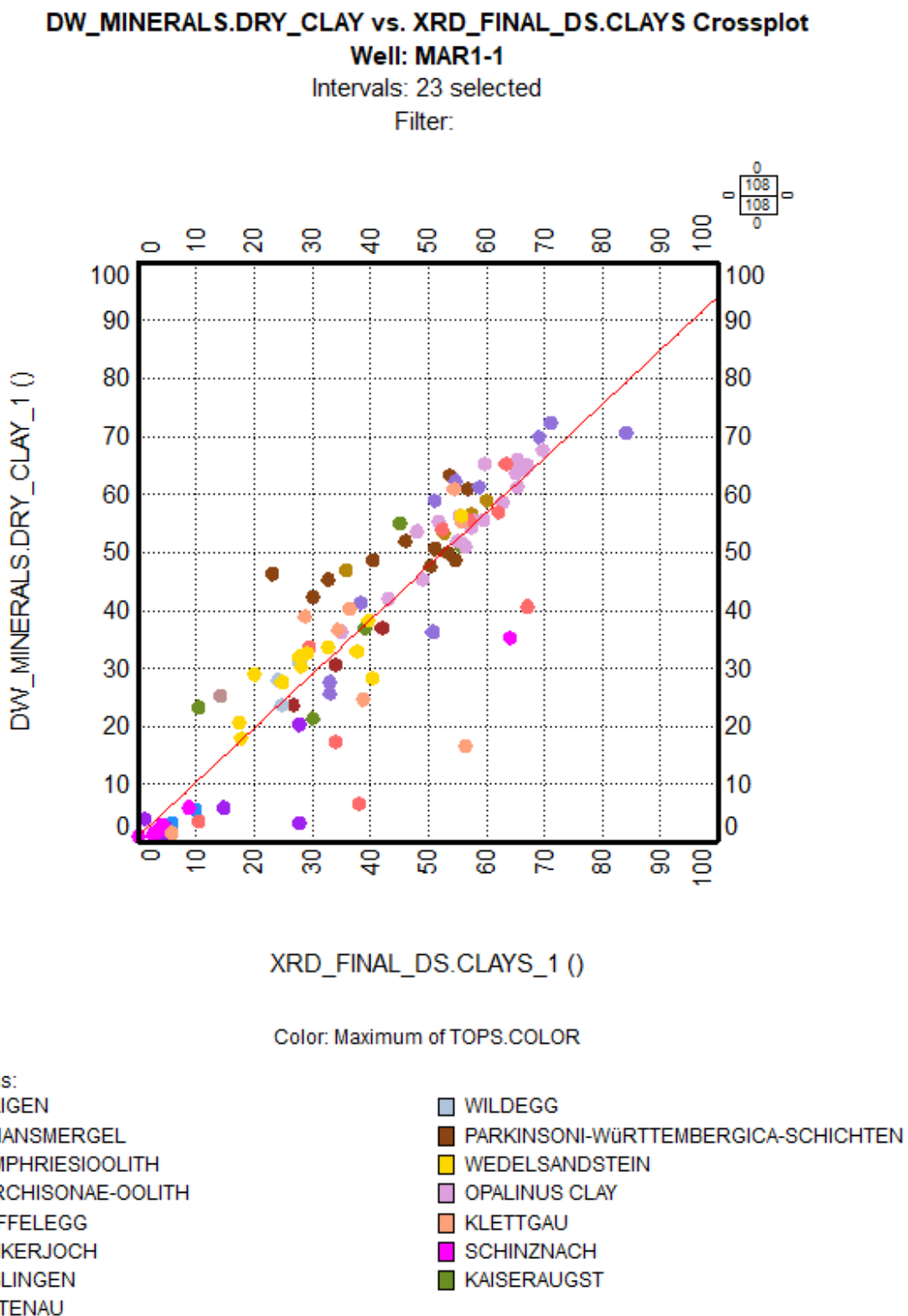


Fig. 4-1: Weight % of dry clay (y-axis) compared to core XRD data (x-axis), Villigen to Weitenau Formations

The MultiMin dry clay content is well correlated to the core XRD data ($cc = 0.91$).

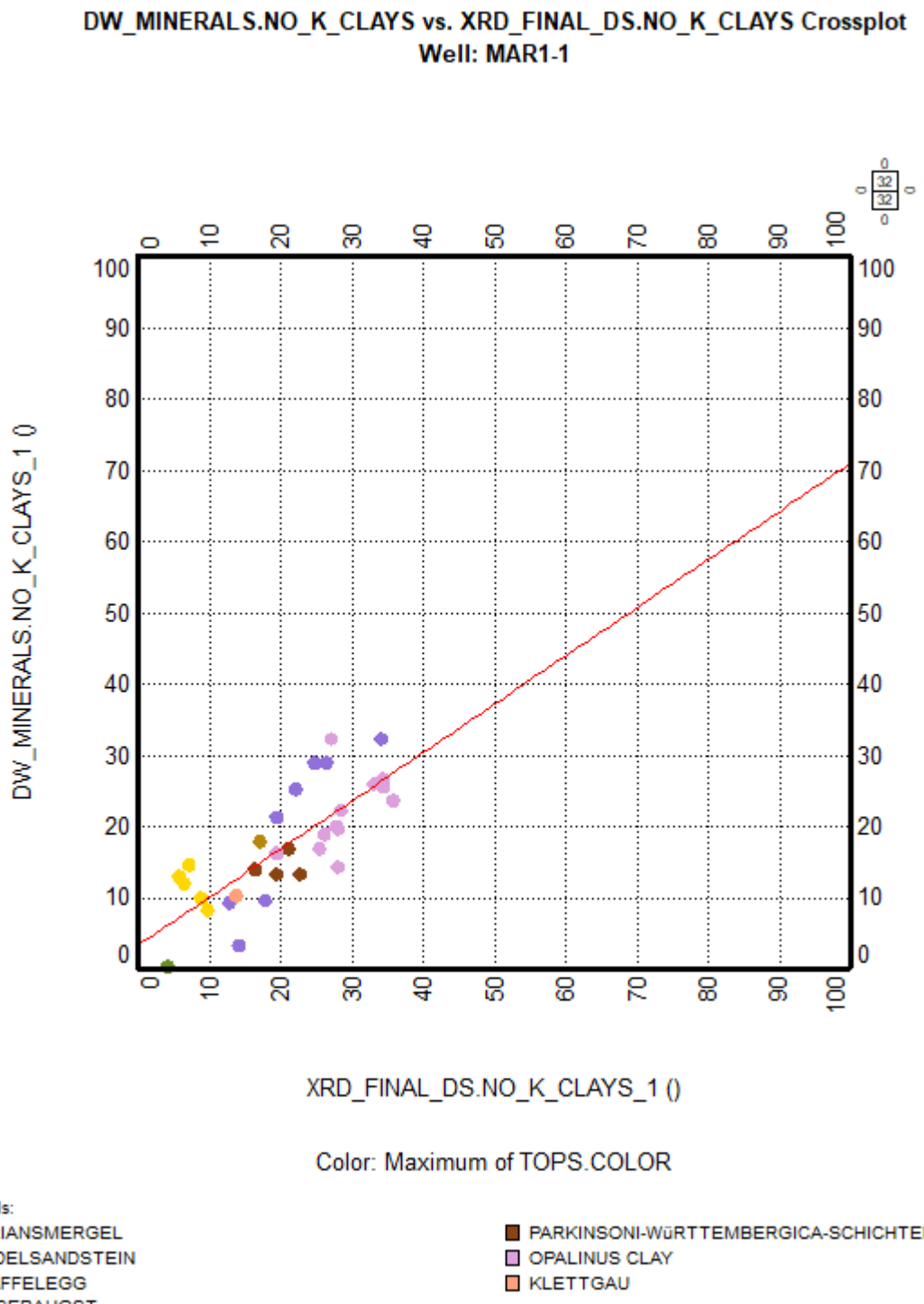


Fig. 4-2: Weight % of not potassic dry clay (y-axis) compared to core XRD data (x-axis), XRD data in the Variansmergel to the Kaiseraugst Formations

The XRD clay endmembers were not measured in all formations.

The MultiMin not potassic clay content is well correlated to the core XRD data in the Opalinus Clay (light purple dots), but overestimated in the «Brauner Dogger» (overall cc = 0.78).

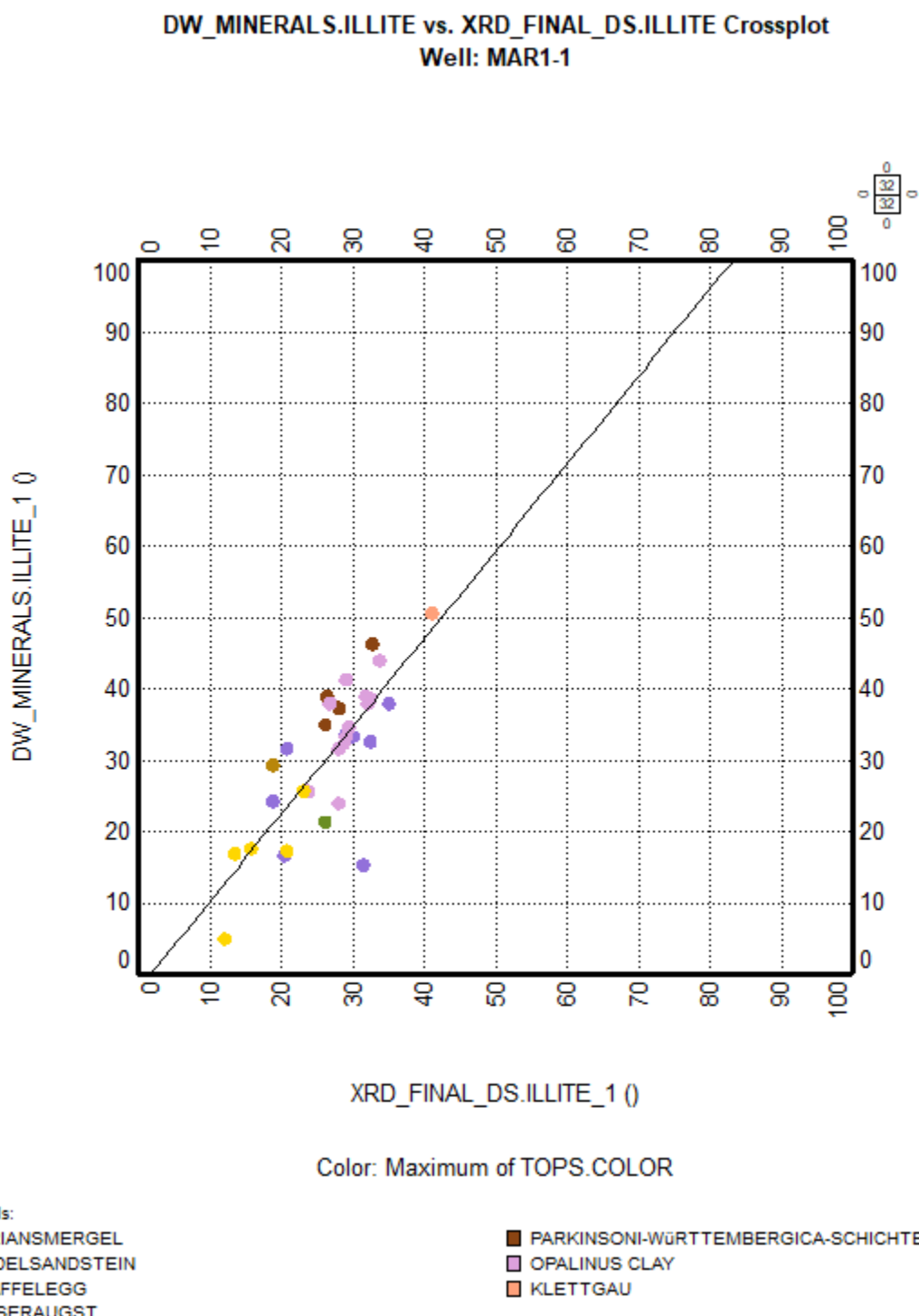


Fig. 4-3: Weight of illite (x axis) compared to core XRD data (y axis), XRD data in the Variansmergel to the Kaiseraugst Formations

The XRD clay endmembers were not measured in all formations.

The MultiMin illite content is fairly correlated to the core XRD data ($cc = 0.78$) but underestimated in the «Brauner Dogger» (yellow and brown dots).

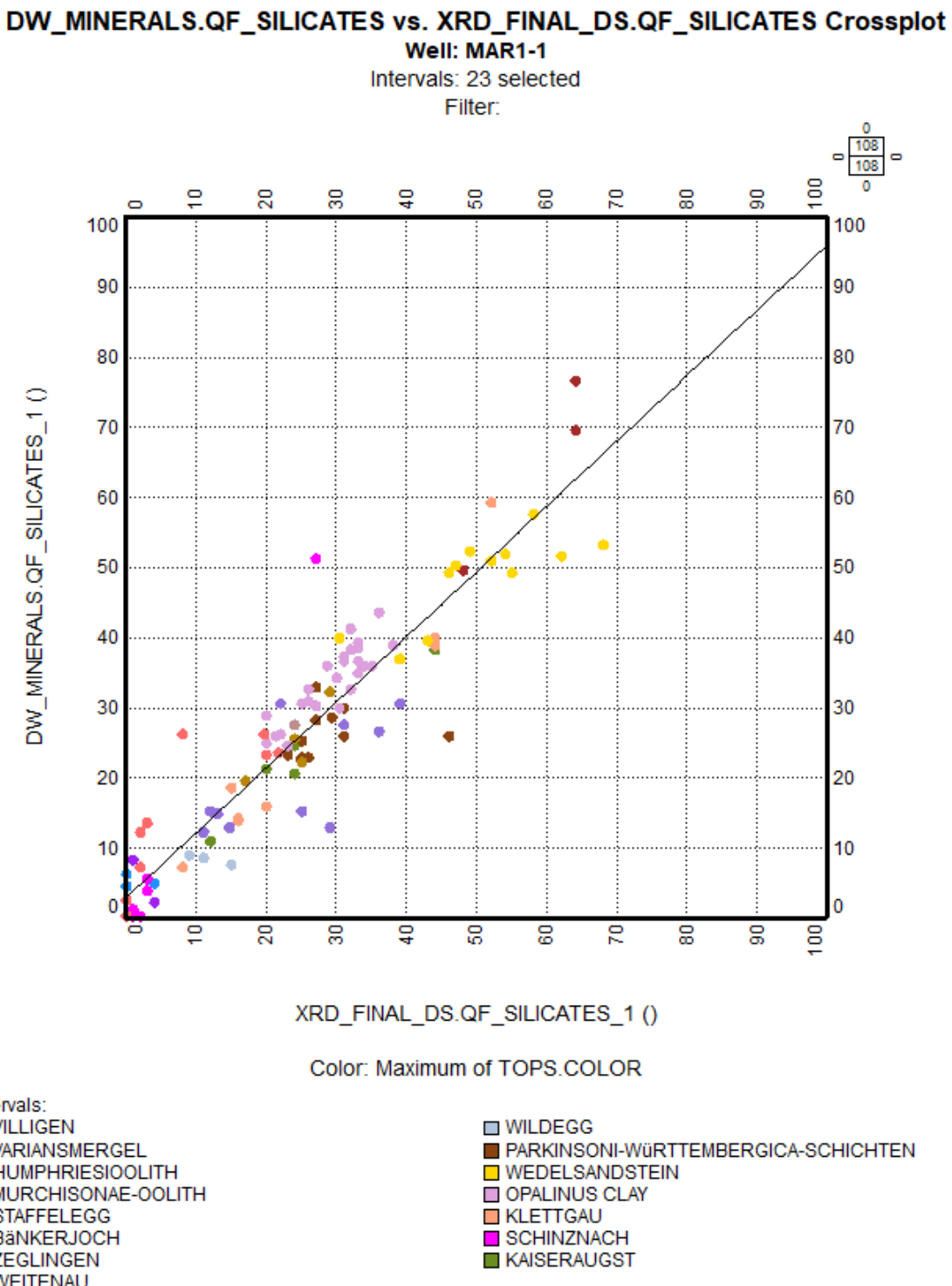


Fig. 4-4: Weight % of QF-silicates (x axis) compared to core XRD data (y axis), Villigen to Weitenau Formations

The QF-silicates are the sum of quartz and feldspars. The calibration to core XRD data is good (cc = 0.93).

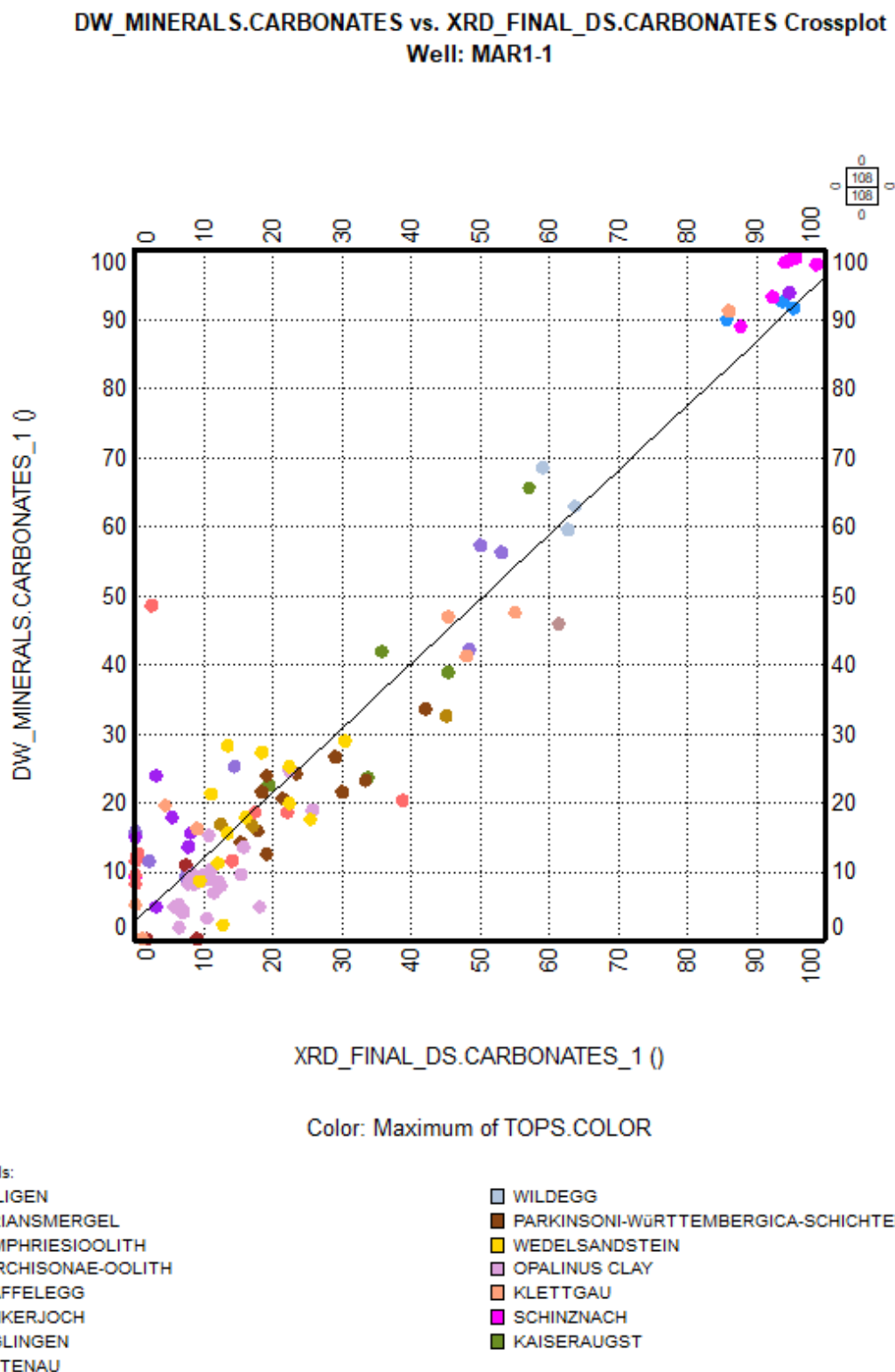


Fig. 4-5: Weight % of carbonates (x axis) compared to core XRD data (y axis), Villigen to Weitenau Formations

The carbonates include the calcite, dolomite and siderite contents. The calibration to core XRD data is good ($cc = 0.95$), despite a few outliers and local heterogeneities.

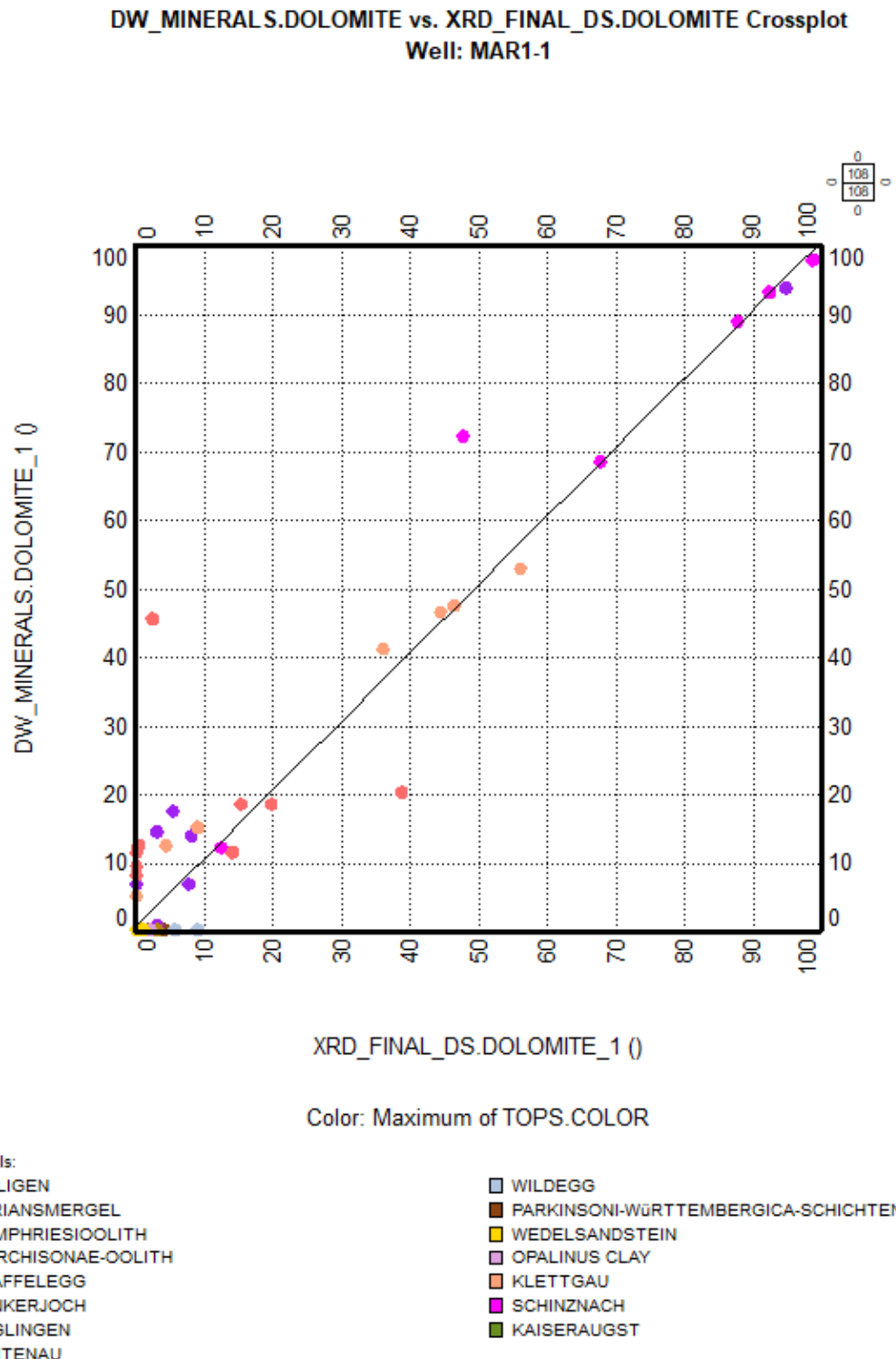


Fig. 4-6: Weight % of dolomite (x axis) compared to core XRD data (y axis), Villigen to Weitenau Formations

The dolostones are mostly located in the Triassic, within complex mineralogical settings including anhydrite. The calibration to core XRD data is good ($cc = 0.96$) but with some dispersion in the dolomitic formations.

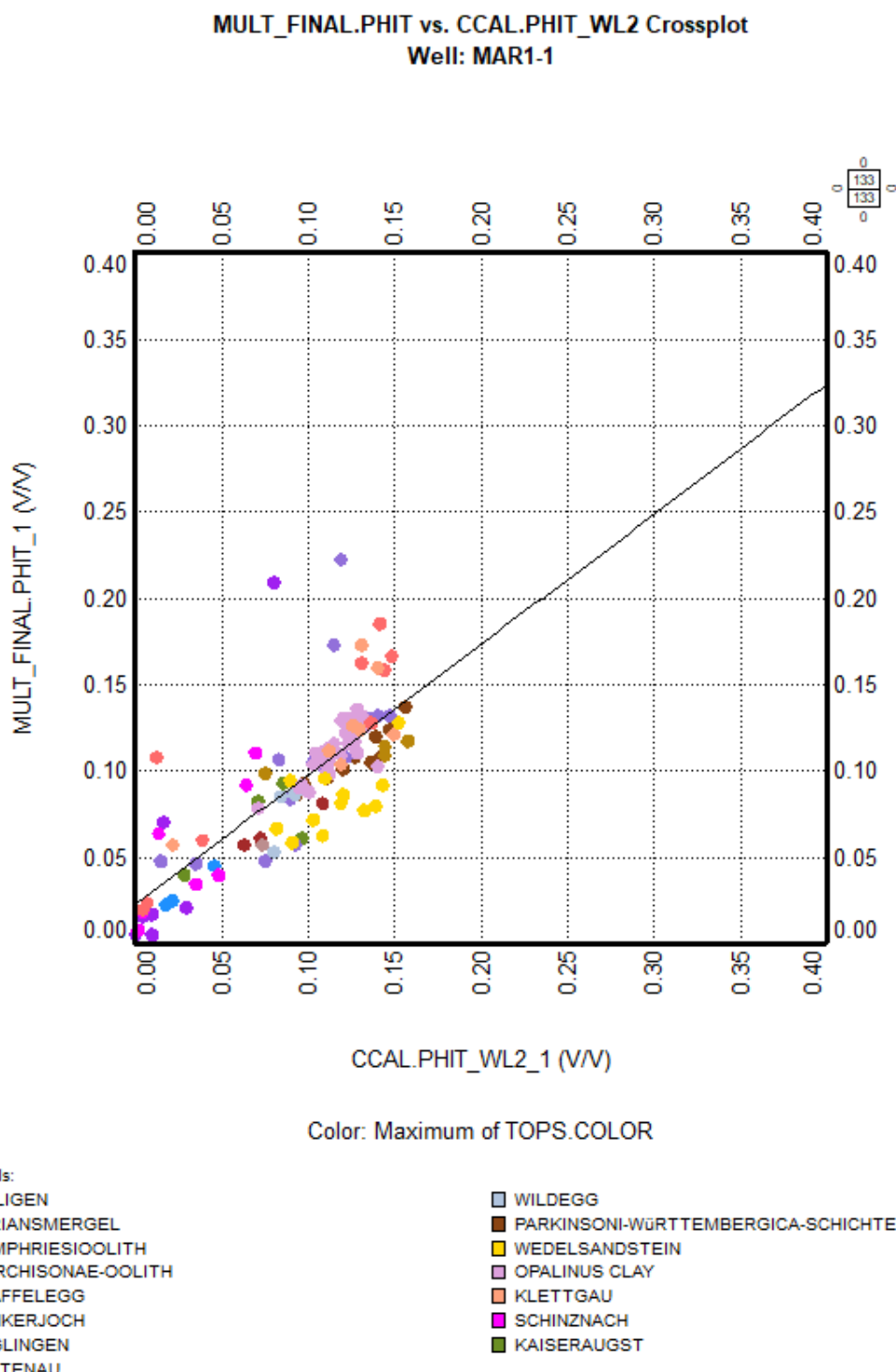


Fig. 4-7: Total porosity (v/v, y axis) compared to core data (x axis), Villigen to Weitenau Formations

The lab porosity used for the comparison was water-loss porosity (105 °C) using grain density at ambient conditions, i.e. no confining stress was applied during measurements. Therefore, cores and log measurements are not fully equivalent as the logs evaluate in situ wet formations. Nevertheless, the correlation between MultiMin and lab porosity is fair ($cc = 0.78$).

MultiMin porosity locally underestimates core porosity, for example in the «Humphriesiolith Formation» and the Wedelsandstein Formation. In this interval, the MultiMin results could not be reconciliated with core porosities, as the core bulk density is lower than the TLD RHOZ, leading to lower MultiMin PHIT.

Inversely, the MultiMin PHIT is likely too high in the Rietheim Member of the Staffelegg Formation, in organic-rich rocks (715.5 – 721 m).

Additionally, some dispersion can be noticed in the Triassic, where the mineralogy is less accurately calibrated to core.

4.2 Main results of the core-calibrated log analysis in borehole MAR1-1

The main aim of the MultiMin interpretation were continuous curves of porosity and clay content of the MAR1-1borehole. Several other minerals have been determined (mainly QF-silicates and carbonates). Below is a summary of the main parameters of clay, carbonate, QF-silicate content and porosity for each system/group.

If not stated otherwise, the clay content is used sensu lato meaning that the clay content is used as a general term for the total clay mineral content of the formation (i.e. the sum of all clay minerals). Carbonates and QF-silicates are also used sensu lato where carbonates are regarded as the sum of all carbonate minerals (calcite, dolomite and siderite) while QF-silicates is used synonymously for the sum of quartz (sensu stricto) and feldspars.

Malm (254.0 – 501.9 m; «Felsenkalke» + «Massenkalk», Schwarzbach Formation, Villigen Formation and Wildegg Formation):

As the 7%" auxiliary casing shoe was installed at 312.0 m MD (Driller), the top part of the Malm could not be logged.

As expected, carbonates are the main constituents in the formations of the Malm, the mean calcite content is 89.9 wt.-% (median of 92.7 wt.-%). Lithological changes (e.g. at group boundaries) are sometimes reflected in a sharp negative peak (i.e. decreasing carbonate content at top Schwarzbach Formation correlated to clay content increase), but in general, the variance of the carbonates in the Malm is low.

Only the Schwarzbach and Wildegg Formations are more argillaceous and correlative less calcareous: respectively 9.2 wt.-% DRY_CLAY and 80.6 wt.-% CALCITE in the Schwarzbach Formation and 21.6% DRY_CLAY and 70.9 wt.-% CALCITE in the Wildegg Formation.

The carbonate content in the Malm is dominated by calcite, as no dolomite was calculated for this group (up to 9 wt.-% on core XRD data in the Wildegg Formation). No siderite was measured on core XRD.

The QF-silicate content in the Malm is low (mean of 5.6 wt.-%, median of 4.9 wt.-%). The more clay-rich lithologies (Schwarzbach and Wildegg Formations) show a slightly increased QF-silicate content (mean / median of the Schwarzbach Formation: 10.1 wt.-% / 10.2 wt.-%, Wildegg Formation: 6.4 wt.-% / 6.7 wt.-%).

Generally, the dry clay content is low (mean of 4.1 wt.-%, median of 1.8 wt.-%) with locally higher values in the more argillaceous intervals (e.g. parts of the Schwarzbach and Wildegg Formations). In the Wildegg Formation, the maximum clay content is close to 42.1 wt.-% with a mean and median of 21.6 wt.-% and 22.7 wt.-%.

Total porosity in the Malm ranges between 0 and 11.8% (mean of 2.9%, median of 2.4%). The highest porosity is observed in the Schwarzbach Formation but must be treated with caution as they might represent artefacts due to a reduced data quality in these intervals.

Dogger (501.9 – 705.5 m, Wutach Formation, Variansmergel Formation, «Parkinsoni-Württembergica-Schichten», «Humphriesoolith Formation», Wedelsandstein Formation, «Murchisonae-Oolith Formation», Opalinus Clay):

The boundary between the Malm and the Dogger is clearly marked by a sharp increase of the iron content (up to 16 wt.-%), the clay content (characterised by a gamma ray peak) and a sharp decrease of the carbonate content to the Wutach Formation.

The carbonate content in the Dogger is generally moderate, with a mean of 16.7 wt.-% and a median of 12.6 wt.-%. The carbonate content is dominated by calcite above the Opalinus Clay (mean / median 25.8 wt.-% / 22.8 wt.-%) and calcite plus siderite in the Opalinus Clay (mean / median calcite 6.5 wt.-% / 5.3 wt.-%; mean / median siderite 2.6 wt.-% / 2.5 wt.-%).

Four calcite-rich thin streaks can be noticed in the upmost half of the Opalinus Clay, visible on the bulk density RHOZ and the calcium content DWCA_WALK2. These streaks are likely not well characterised due to the limited vertical resolution of the ECS tool.

When comparing the ECS iron content (corrected to XRF data, DWFE_CORR curve) with the XRD iron-rich minerals in the «Brauner Dogger», an excess of iron can be noticed. If the iron content measurement is valid, the presence of an additional iron-rich mineral species is possible. This was modelled as iron oxide with MultiMin.

The QF-silicate content in the Dogger ranges between 1.1 wt.-% and 59.9 wt.-%. The mean and median values (32.4 wt.-% and 31.9 wt.-%) are heavily influenced (increased) by the Wedelsandstein Formation (mean / median 44.3 wt.-% / 45.3 wt.-%) and the thin «Murchisonae-Oolith Formation», while the other formations are in the range between 1.1 wt.-% and 49.8 wt.-%.

The Opalinus Clay in the Dogger certainly is the formation with the highest clay content, ranging between 29.8 wt.-% and 74.4 wt.-% (mean / median of 55.9 wt.-% / 55.8 wt.-%). The clay content is high but variable in the formations above (minimum 12.6 wt.-%, maximum 73.3 wt.-%, mean / median of 40.8 wt.-% / 41.9 wt.-%).

Total porosity of the Dogger also is contrasted between the different units. PHIT is not very variable in the Opalinus Clay (minimum / maximum 6.5% / 14.3%, mean and median both 11.2% with a low standard deviation of 1.5%). It is more variable in the overlying Dogger formations (minimum / maximum 4.2% / 24.7%, mean / median 9.1% and a standard deviation of 2.6%). This maximum computed value of 24.7% corresponds to a dubious spike in an iron-rich streak within the «Humphriesoolith Formation», which should be regarded as artefact from the MultiMin interpretation (the quality indicator is above 2, suggesting a less reliable model).

It must be reminded that the MultiMin PHIT could not be calibrated with the core porosity in the Variansmergel Formation to Wedelsandstein Formation. The MultiMin PHIT is often lower than the core PHIT in this interval. This difference is related to a higher wireline logs bulk density (RHOZ curve) when compared to core bulk density. The crossplot in Fig. 4-8 illustrates this discrepancy between wireline and core data.

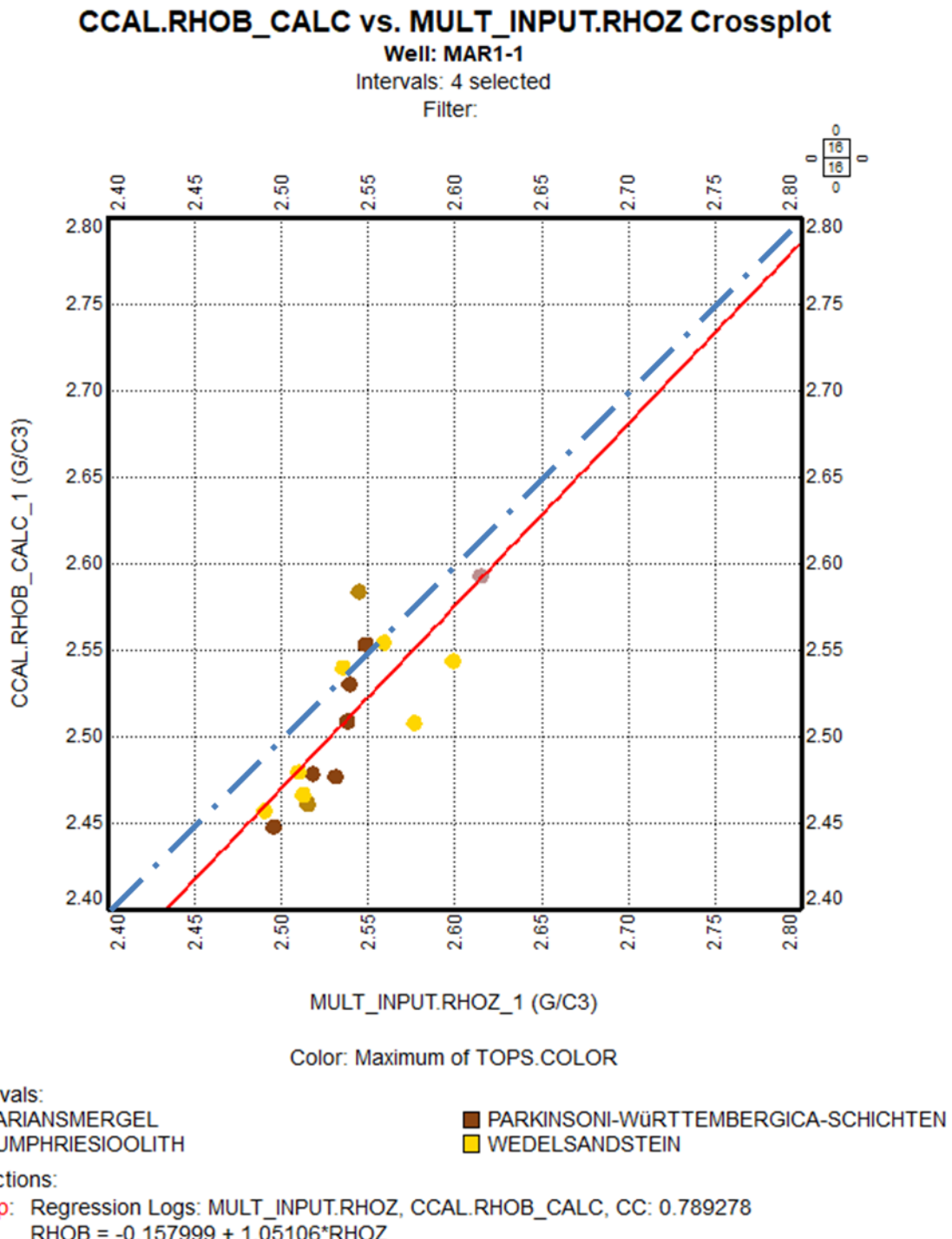


Fig. 4-8: Bulk density computed from core grain density and water loss porosity versus RHOZ in the «Brauner Dogger»

The lab porosity used for the comparison was water-loss porosity (105 °C) using grain density at ambient conditions, i.e. no confining stress was applied during measurements. The core bulk density was computed from the grain density and the water loss porosity using the following equation: $RHOB_CALC = PHIT * 1.03 + (1-PHIT) * RHOG$

The fluid density is 1.03 g/cm³, corresponding to brine salinity at temperature and pressure. This crossplot shows a higher bulk density measured by the wireline logs, causing the mismatch between core and log porosity in the «Brauner Dogger». At this stage it is not possible to state if the log porosity is too low or the core porosity too high.

Lias (705.5 – 747.9 m, Staffelegg Formation):

The formation boundary from the Opalinus Clay (Dogger) to the Staffelegg Formation (Lias) corresponds to a sharp drop of the clay content and a sharp rise of the carbonate (mostly calcite) content.

The carbonate content of the Lias reflects the lithology where the upper parts (Gross Wolf down to Grünschholz Members) have a relatively high carbonate content (up to 80.0 wt.-%), while the lower part (Frick to Schambelen Members) have a relatively lower carbonate content (mean / median 23.0 wt.-% / 11.6 wt.-%). As in the previous groups, the carbonate content is dominated by calcite, no dolomite content has been calculated or measured from cores. Low siderite content was measured from cores (up to 2.9 wt.-%) but could not be modelled with MultiMin.

The QF-silicate content shows the reverse of the carbonate content. While the upper part (Gross Wolf down to Grünschholz Member) shows a relatively low QF-silicate content (mean / median 10.7 wt.-% / 9.5 wt.-%), the lower part (Frick to Schambelen Members) shows higher QF-silicate contents (mean / median 25.2 wt.-% / 29.0 wt.-%).

The clay content follows the same trend, moderate in the upper part (mean / median 32.1 wt.-% / 32.6 wt.-%) and high in the lower half (mean / median 49.8 wt.-% / 56.8 wt.-%).

The Staffelegg Formation is also characterised by high total organic carbon (TOC), not fully reconstructed by the MultiMin interpretation with the available wireline logs. The maximum TOC measured on cores was 6.74 wt.-% at 720.33 m. This miscalibration of the TOC impacts the PHIT computation.

The total porosity in the Staffelegg Formation ranges from 2.2% to 24.7%, the highest values in the Rietheim Member likely being artefacts due to the poor calibration of the high TOC. Except in this member, the total porosity increases with the clay content, up to 12% at the base of the Frick Member.

The mean / median PHIT in the Staffelegg Formation are 9.6% / 10.0%.

Keuper (747.9 – 862.8 m, Klettgau Formation, Bänkerjoch Formation):

In the Keuper, the top part of the Klettgau Formation (Gruhalde and Seebi Members) is characterised by a complex mineralogical mixture of carbonates (mostly dolomite) between 0 and 91.3 wt.-% (the latter represents calcitic dolostones within the Seebi Member), QF-silicates (quartz and feldspars) between 0 and 66.4 wt.-% and clays (dominant illite) between 0 and 75.3 wt.-%. The base of the Seebi Member is a sandstone, up to 66.4 wt.-% QF-silicates.

The Gansingen Member is an anhydrite bed, while the base Klettgau Formation (Ergolz Member) is an argillaceous formation (20 wt.-% to 68.9 wt.-% clays, mean 52.4 wt.-%) with QF-silicates (11.6 wt.-% to 57.8 wt.-%, mean 30.9 wt.-%).

The underlying Bänkerjoch Formation is dominated by anhydritic deposits: 0 to 99.8 wt.-% (mean 37.7 wt.-%). In complement, carbonates (dolomite), clays and QF-silicates are well represented in this formation.

The total porosity ranges from 0 to 21.6% (mean 10.2% and median 10.7%). The lowest porosities correspond to the anhydrites, while the highest ones are dubious in the rugose borehole (flagged with MULT_QC = 2).

The wireline log quality is often good in the Keuper, with a locally slightly enlarged caliper (up to 8.4" in a 6 $\frac{3}{8}$ " borehole) and HDRA above 0 g/cc suggesting local wall rugosity. The MultiMin results are more limited by the low log redundancy versus complex mineralogical mixtures, leading to a quality indicator often above 1.

Muschelkalk (862.8 – 1'030.0 m, Schinznach Formation, Zeglingen Formation, Kaiseraugst Formation):

The magnesium content was measured with the MGWALK closure model, which helped characterising the dolomite content of the Muschelkalk.

The boundary from the Keuper to the Muschelkalk is marked by a sharp increase of the carbonate content which here is dolomite. The Asp and Stamberg Members are mostly dolomitic (except for a thin peak of QF-silicate and clay content in the uppermost part of the Muschelkalk, base Asp Member), while the top of the Liedertswil Member is a progressive transition to dolomitic limestones, then limestones at the bottom of the Leutschenberg/Kienberg Members.

The carbonate content of the Schinznach Formation ranges from 7.6 wt.-% to 100 wt.-% (mean 93.6 wt.-%, median 96.6 wt.-%): mean 88.3 wt.-% dolomite in the Asp and Stamberg Members at the top, 37.7 wt.-% dolomite and 59.5 wt.-% calcite in the Liedertswil and Leutschenberg/Kienberg Members at the base.

The top Zeglingen Formation is characterised by a sharp decrease of the calcite content, replaced by dolomite. The anhydrite content, well picked up by the ECS DWSU_WALK2 curve, increases downwards in the Dolomitzone Member, while the Sulfatzone Member is mostly anhydritic.

A sharp anhydrite to carbonates and clays transition indicates the top Kaiseraugst Formation, with a complex mineralogical mixture of carbonates, QF-silicates and clays: mean 31.3 wt.-% carbonates, 22.2 wt.-% QF-silicates and 40.0 wt.-% clays. A thin anhydritic bed is seen at the base of the Orbicularismergel Member.

Total porosity in the Muschelkalk is very variable and ranges from 0 to 29.6%. This highest value within the dolostones of the Dolomitzone Member at the top Zeglingen Formation coincides with an enlarged and rugose borehole and is therefore dubious; it was flagged by the MULT_QC curve.

The lowest porosity rocks are the anhydrites and the dolomitic limestones in the Liedertswil and Leutschenberg/Kienberg Members at the base of the Schinznach Formation.

Buntsandstein (1'030.0 – 1'038.3 m, Dinkelberg Formation) and **Rotliegend** (1'038.3 – 1'094.1 m, Weitenau Formation):

The number of available wireline logs data in the Weitenau Formation is gradually reduced below the first readings below approximately 1'049 m. Neither ECS, APS nor HNGS were acquired in the section below. The mineralogical model was therefore simplified to clays and QF-silicates.

The boundary from the Muschelkalk to the sandstones of the Buntsandstein and Rotliegend is characterised by a sharp increase of the QF-silicate content and a sharp decrease of the carbonate and clay contents. On the logs this corresponds to a sharp gamma ray decrease.

The QF-silicate content is high in the Buntsandstein (mean / median of 71.8 wt.-% / 80.0 wt.-%) and in the Rotliegend (mean / median: 73.5 wt.-% / 74.4 wt.-%).

An increased carbonate content is computed at the base of the Dinkelberg Formation, driven by the ECS calcium content (mean / median 15.8 wt.-% / 2.6 wt.-%, maximum 65.0 wt.-%). The carbonate content in the Weitenau Formation is very low (mean / median 0.3 wt.-% / 0.5 wt.-%).

The clay content in the Buntsandstein (mean / median: 12.4 wt.-% / 12.9 wt.-%, maximum 18.4 wt.-%) is lower than in the Rotliegend (mean / median: 26.1 wt.-% / 25.5 wt.-%, maximum 36.4 wt.-%).

Total porosity in the Buntsandstein ranges from 1.6% to 20.8% (mean 10.0%, median 9.8%), while it is lower in the Rotliegend: 4.2% to 7.2% (mean and median 5.9%).

Crystalline Basement (1'259.7 – 1'310.0 m):

This interval was not interpreted in this study, due to the lack of logs coverage.

4.3 Main results of the core-calibrated log analysis in the Opalinus Clay (590.4 – 705.5 m)

The main results in terms of total clay content, mineralogy and total porosity for the main focus interval (Opalinus Clay) are shortly described in this section. Figs. 4-9 to 4-15 show some general statistical values of the MultiMin analysis results within the Opalinus Clay.

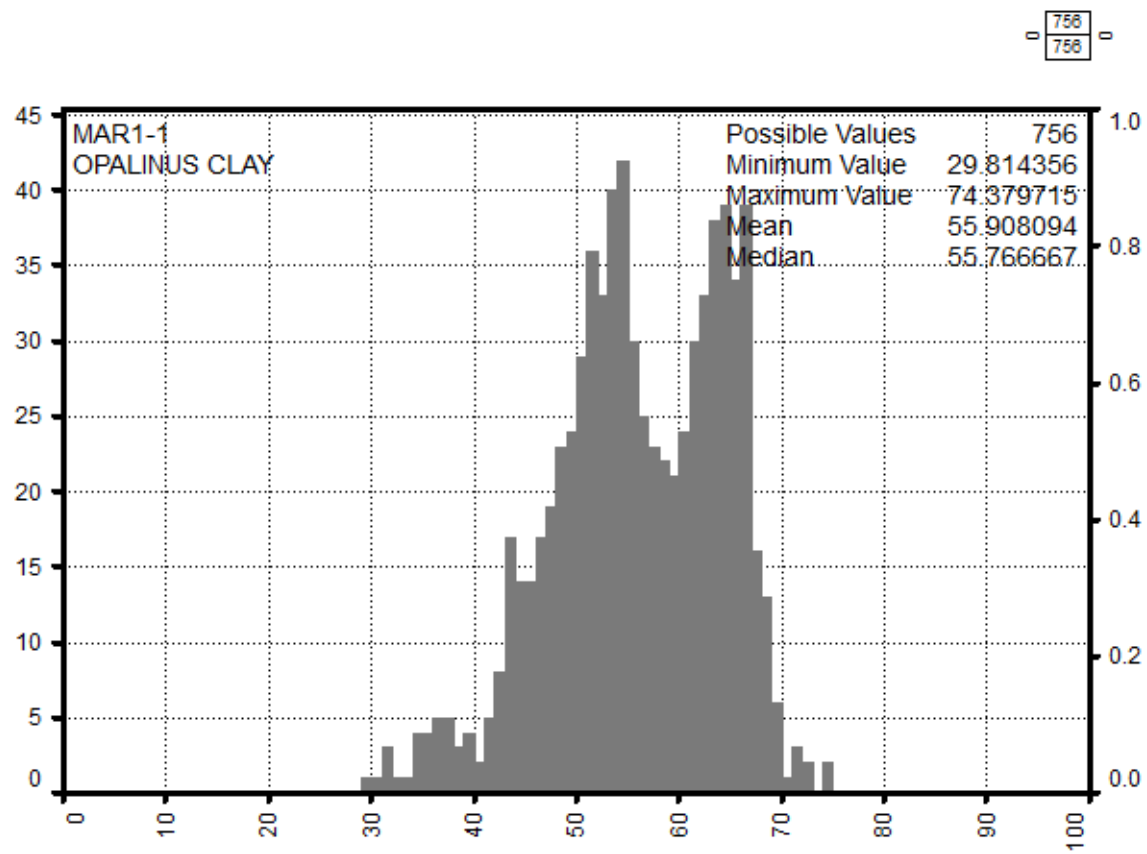


Fig. 4-9: Dry clay weight percentage frequency histogram in the Opaline Clay
X axis is the dry clay weight % from MultiMin, y axis the number of points (100 bins).

In the clay-rich Opalinus Clay, the mean and median dry clay contents are close to 59.7 wt.-%. The distribution looks bimodal, with the lowest clay content in the shallowest part of the Opalinus Clay).

The two next frequency histograms show a split of the Opalinus Clay into an upper and lower part, showing that the latter is slightly more argillaceous.

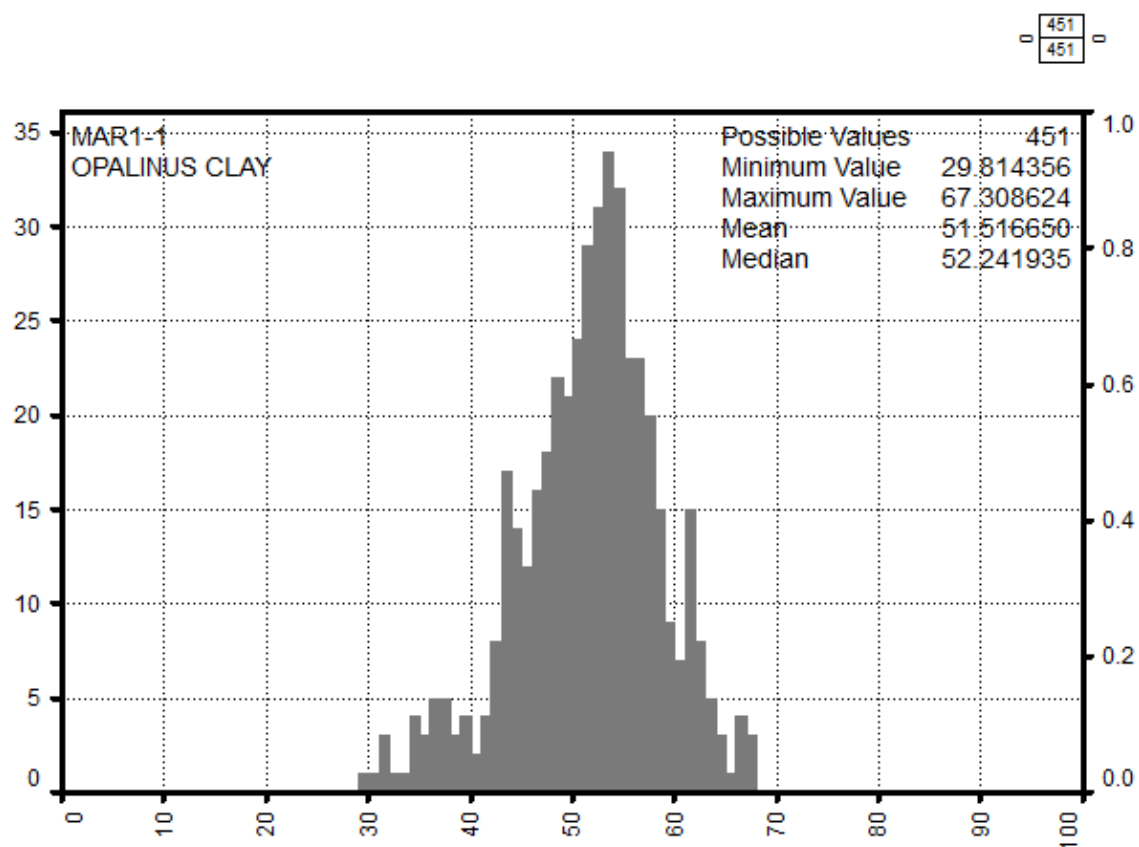


Fig. 4-10: Dry clay weight percentage frequency histogram in the upper section of the Opalinus Clay (above 659 m)

X axis is the dry clay weight % from MultiMin, y axis the number of points per bin (100 bins).

In the upper part of the Opalinus Clay (above 659 m), the mean and median dry clay content are close to 51.5 wt.-% and 52.2 wt.-%. The top part of the formation is significantly less argillaceous than the bottom, see next figure.

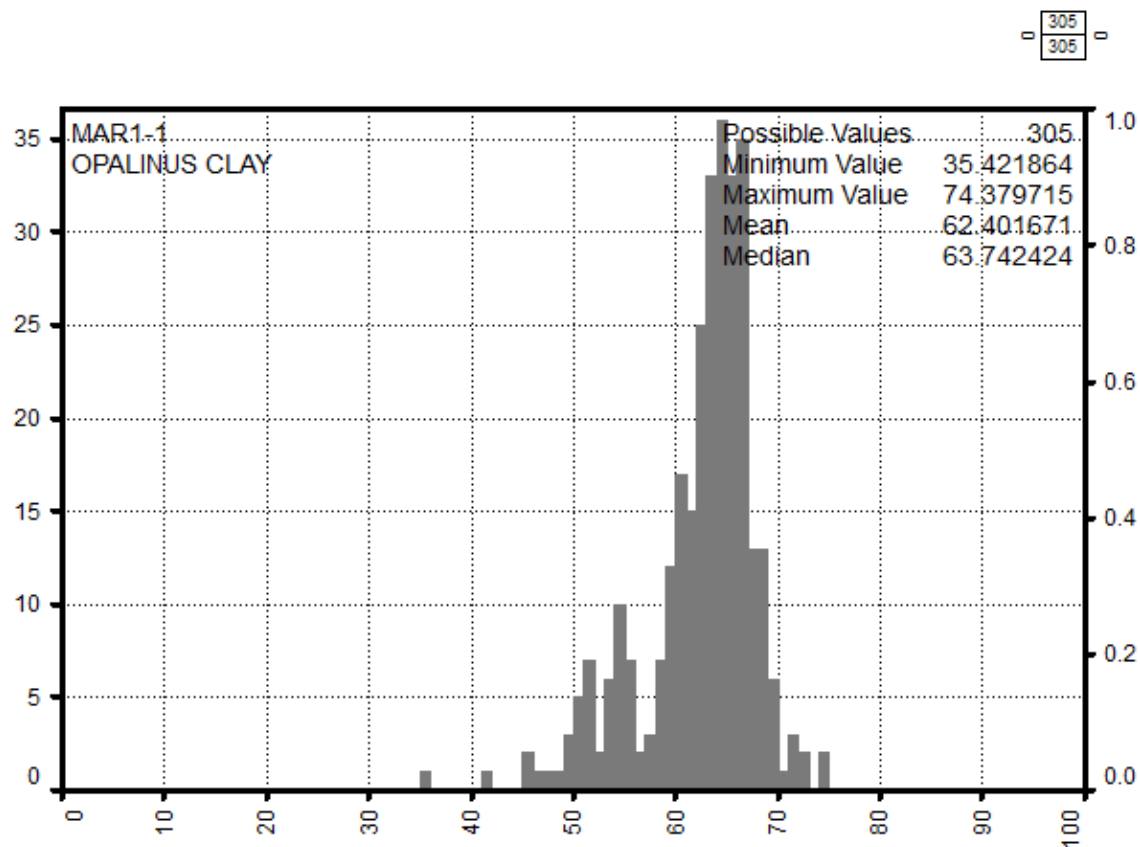


Fig. 4-11: Dry clay weight percentage frequency histogram in the lower section of the Opalinus Clay (below 659 m)

X axis is the dry clay weight % from MultiMin, y axis the number of points per bin (100 bins).

The bottom part of the Opalinus Clay (below 659 m) is more argillaceous: the mean and median dry clay content are close to 62.4 wt.-% and 63.7 wt.-%.

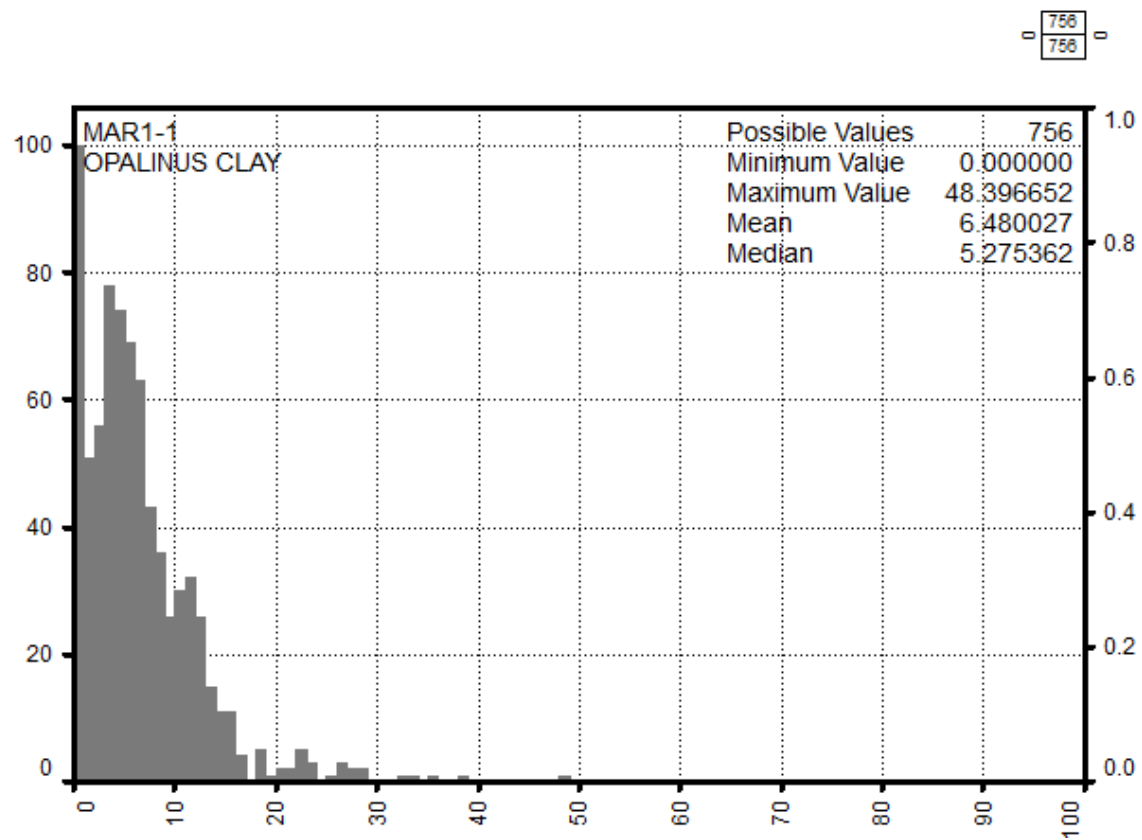


Fig. 4-12: Calcite weight percentage frequency histogram in the Opalinus Clay
X axis is the calcite weight % from MultiMin, y axis the number of points per bin (100 bins).

The mean and median calcite content are close to 6.5 wt.-% and 5.3 wt.-%. The maximum values are up to 48.4 wt.-%, i.e. corresponding to thin, calcite-rich layers. In case these layers are thinner than the log resolution, the maximum calcite content would be higher than computed by MultiMin.

The top part of the Opalinus Clay is more calcitic than the bottom, see Plates 1 and 2.

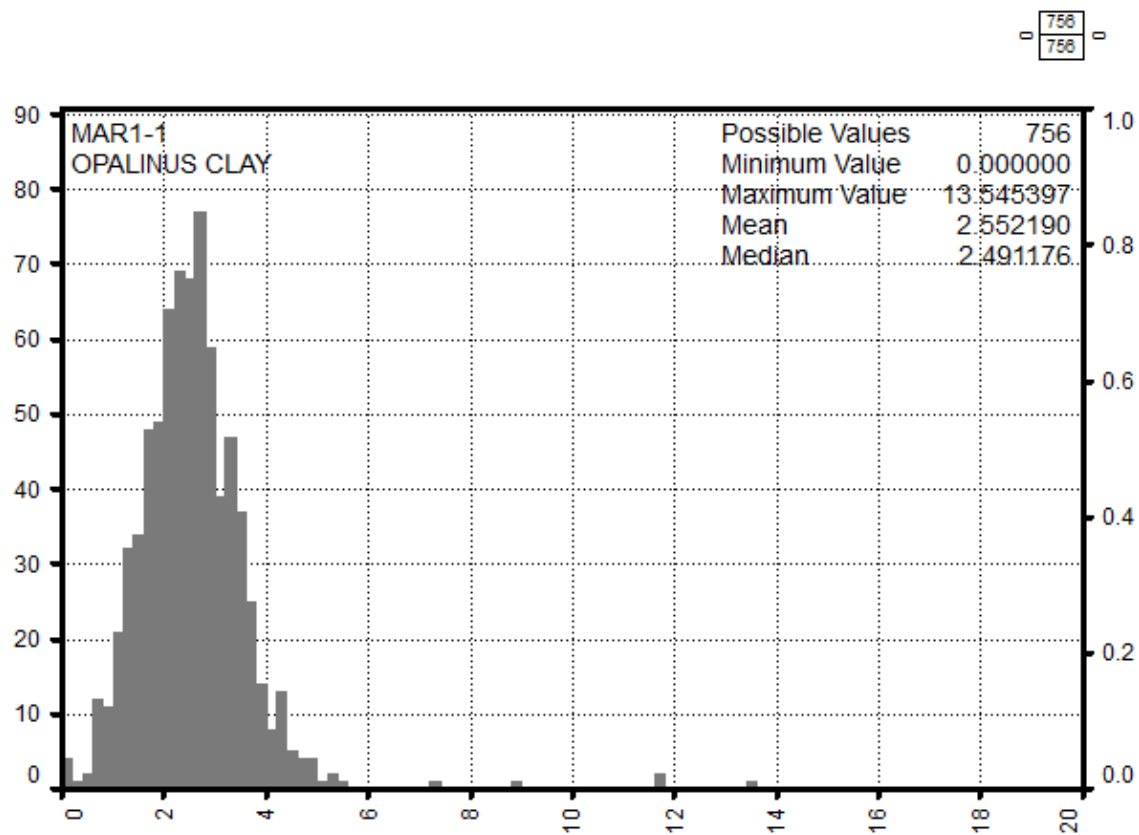


Fig. 4-13: Siderite weight percentage frequency histogram in the Opalinus Clay
X axis is the siderite weight % from MultiMin, y axis the number of points per bin (100 bins).

The mean and median siderite content are close to 2.5 wt.-%, with a maximum value of 13.5 wt.-% and minimum values close to 0 wt.-%. Please note that the siderite core calibration is less constrained than other minerals.

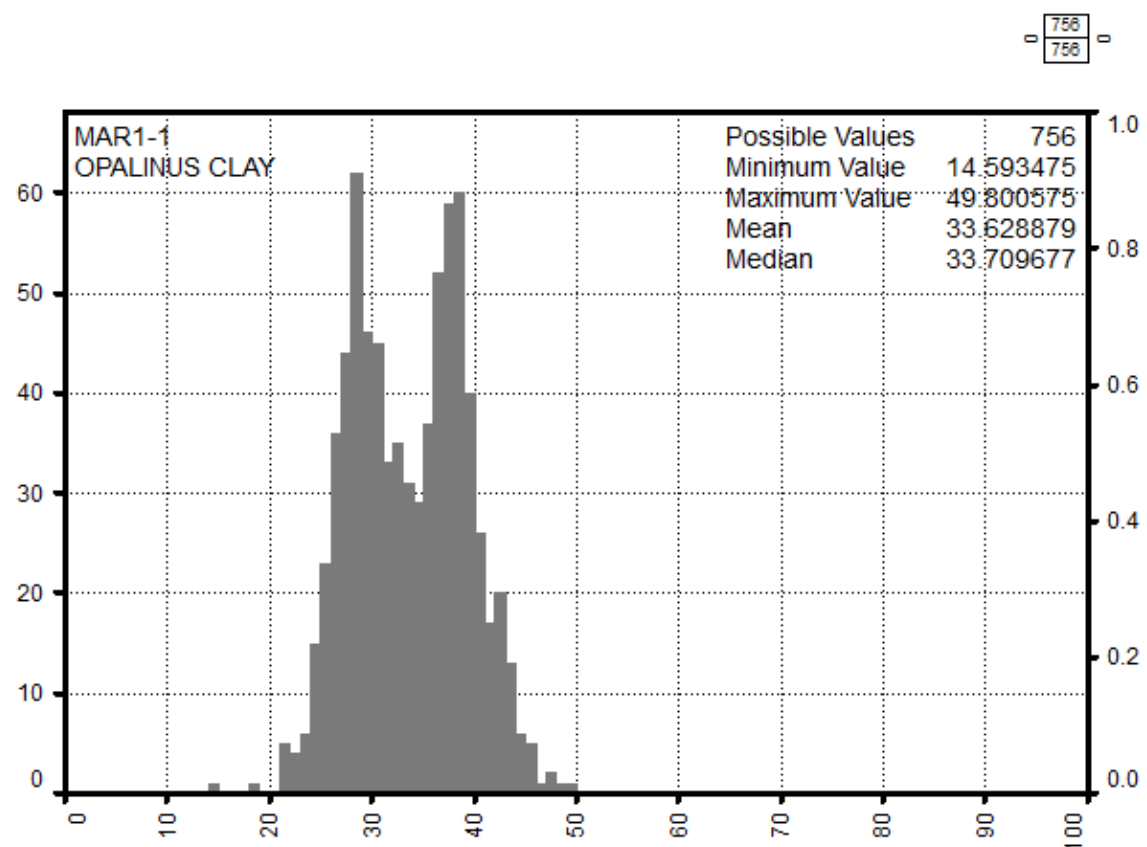


Fig. 4-14: QF-silicates (quartz and feldspars) weight percentage frequency histogram in the Opalinus Clay

X axis is the QF-silicates weight % from MultiMin, y axis the number of points per bin (100 bins).

The mean and median QF-silicates (quartz, plagioclases and potassic feldspars) contents are close to 33.6 wt.-%, much higher than the carbonates (calcite close to 5 wt.-% / 6 wt.-%).

From core XRD data, the quartz represents two thirds and feldspars the remaining third.

The distribution is bimodal, the higher silicates content being in the top part of the formation.

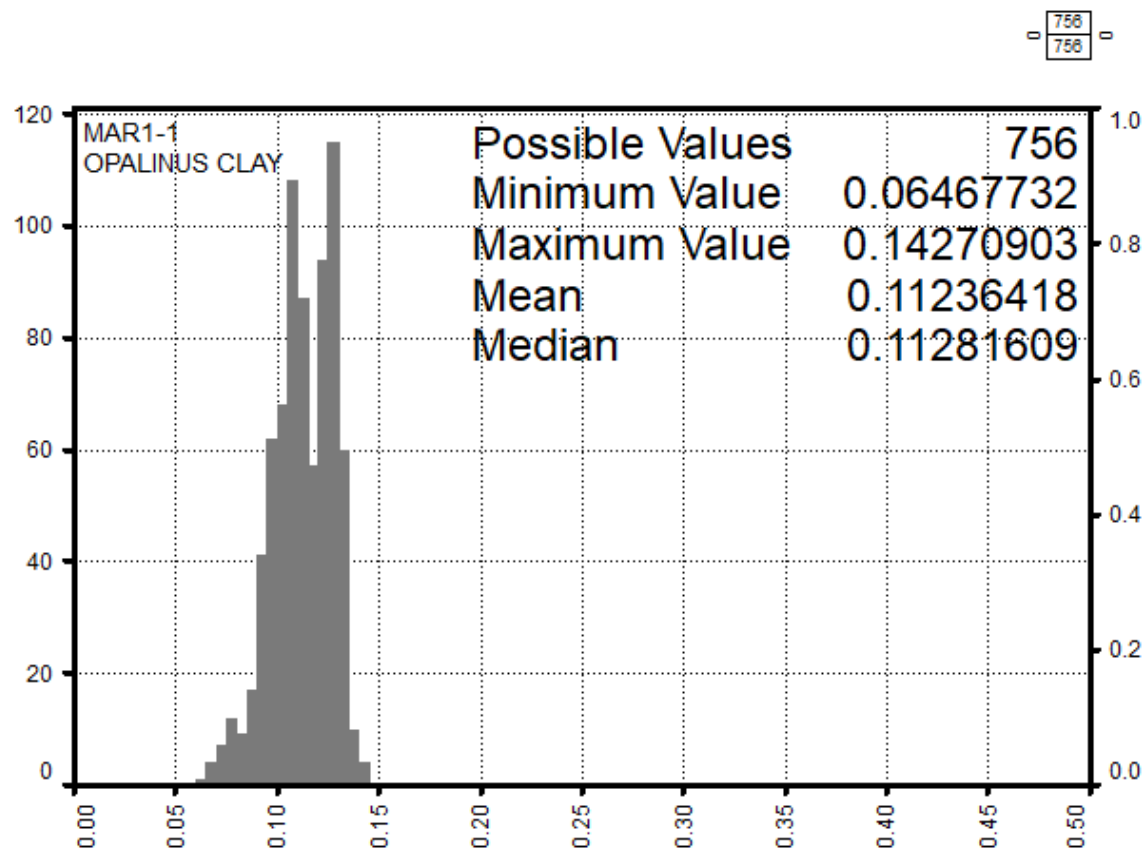


Fig. 4-15: Total porosity frequency histogram in the Opalinus Clay
X axis is the total porosity v/v from MultiMin, y axis the number of points per bin (100 bins).

The mean and median total porosities are close to 11.2%, with a range from 6.5% to 14.3%. The distribution is bimodal, reflecting the distribution of the clay content.

Fig. 4-16 summarises the main results in the Opalinus Clay.

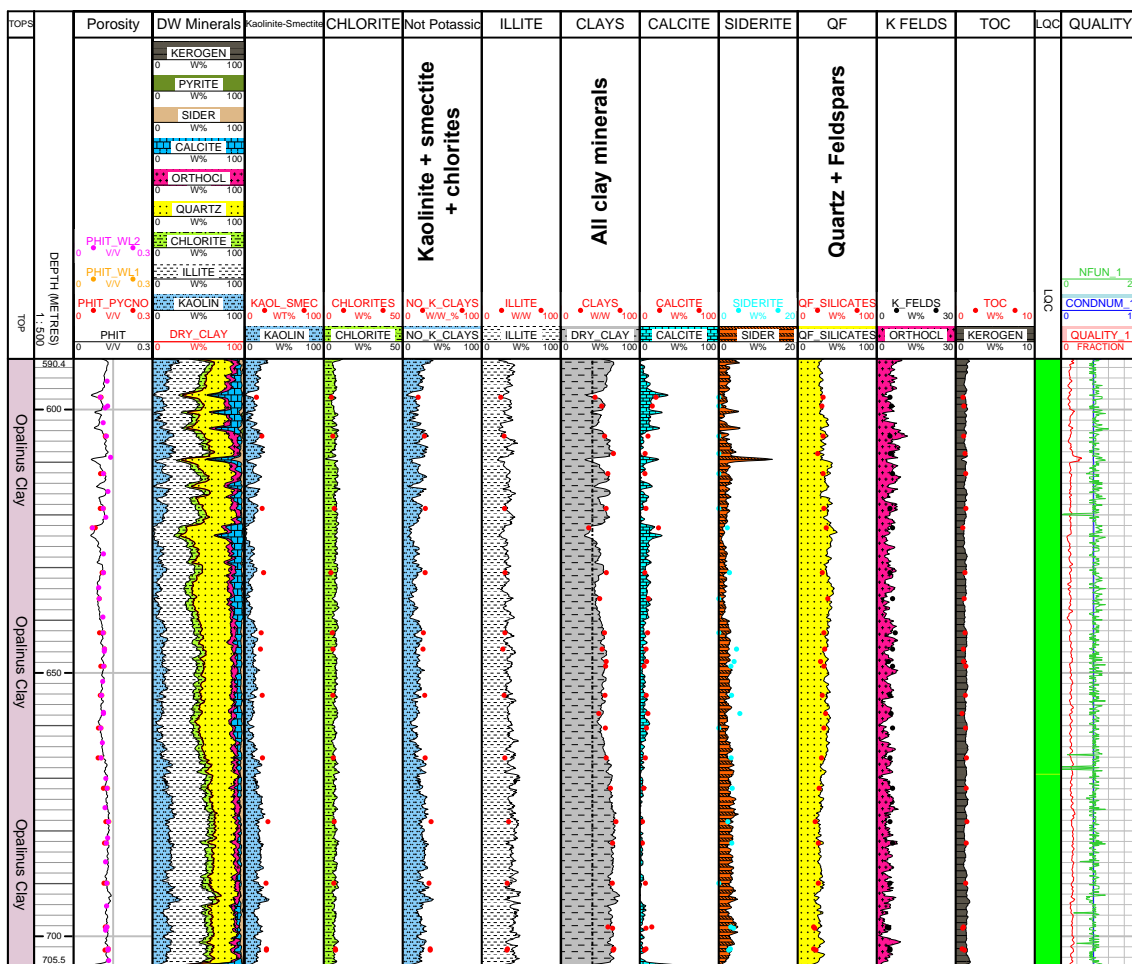


Fig. 4-16: Main log and core results in the Opalinus Clay

The black line in the All clay minerals track represents a 40% baseline.

The wireline log quality was good in all the Opalinus Clay, as shown by the green LQC flag.

The MultiMin quality curve always remains low, generally below 1.00, indicating an overall good curve prediction.

The total porosity and the main minerals dry weight are well calibrated to the core XRD measurements. The siderite and TOC calibration are less accurate.

The whole Opalinus Clay is very argillaceous, almost always above the 40 wt.-% (black line in the "All clay minerals" track in Fig. 4-16). A few carbonates streaks in the top third part have a lower clay content.

5 Summary

The MultiMin interpretation was successfully applied in the MAR1-1 borehole using the Paradigm Geolog MultiMin software (see Plates 1 and 2). Based on available petrophysical logs and formation mineralogical contents, several specific MultiMin interpretation intervals were identified. Some of these intervals needed to be further subdivided due to e.g. borehole conditions to ensure the best possible MultiMin interpretation result.

Core data from lab measurements were also available so that the mineralogical content and other parameters (e.g. density and/or porosity) were known at several points along the borehole. These core data included bulk rock XRD mineralogy, clay mineralogy, pycnometer and water loss porosity as well as grain density. The core data was used as a starting parameter set for the MultiMin interpretation where available.

The mineralogical MultiMin interpretation results were converted to weight percentages for a straightforward comparison with core XRD measurements. In general, the comparisons showed a good agreement between the mineralogy (and porosity) from the MultiMin interpretation and the core data. QF-silicates and carbonates show a good agreement with core data throughout the borehole even in the lowermost units. The differentiation between illite (potassic clay) and non-potassic clays was fairly achieved, while the chlorite endmember remains less accurate. The total porosity is well calibrated to core measurements in the Opalinus Clay; the calibration was fair in the whole borehole, with occasional miscalibrations where the borehole quality was degraded (e.g. in the Keuper), in organic-rich layers of the Staffelegg Formation and in the «Brauner Dogger» (core PHIT higher than MultiMin PHIT as core-derived bulk density is lower than from logs).

The continuous curves from the MultiMin interpretation can be used to characterise the different formations (and hence members) occurring in MAR1-1. The Opalinus Clay shows a quite variable total clay content, though in most locations it is well above 40 wt.-%. The lower third of the formation is significantly more argillaceous than the top, as already noticed in many regional locations.

In addition, boundaries between formations (and between members) are often clearly marked by a decrease or increase of clay, QF-silicate and/or carbonate content. The carbonate-rich formations can further be characterised according to the occurrence of dolomite (replacing calcite), especially in the lower part of the borehole (in the lithostratigraphic units of the Keuper and Muschelkalk). The recent measurement of the magnesium content with the ECS tool (MGWALK closure model) greatly supported the calcite – dolomite characterisation in these formations.

6 References

- Isler, A., Pasquier, F. & Huber, M. (1984): Geologische Karte der zentralen Nordschweiz 1:100'000. Herausgegeben von der Nagra und der Schweiz. Geol. Komm.
- Marnat, S. & Becker, J.K. (2021): Petrophysical log analyses of deep and shallow boreholes: methodology report. Nagra Arbeitsbericht NAB 20-30.
- Mazurek, M. (2017): Gesteinsparameter-Datenbank Nordschweiz – Version 2. Nagra Arbeitsbericht NAB 17-56.
- Nagra (2014): SGT Etappe 2: Vorschlag weiter zu untersuchender geologischer Standortgebiete mit zugehörigen Standortarealen für die Oberflächenanlage. Geologische Grundlagen. Dossier II: Sedimentologische und tektonische Verhältnisse. Nagra Technischer Bericht NTB 14-02.
- Pietsch, J. & Jordan, P. (2014): Digitales Höhenmodell Basis Quartär der Nordschweiz – Version 2013 (SGT E2) und ausgewählte Auswertungen. Nagra Arbeitsbericht NAB 14-02.
- Waber, H.N. (ed.) (2020): SGT-E3 deep drilling campaign (TBO): Experiment procedures and analytical methods at RWI, University of Bern (Version 1.0, April 2020). Nagra Arbeitsbericht NAB 20-13.